Device to Transmit Critical Information from the Interior of a Spent Fuel Cask

By:

Mark Massie (Coordinator)
Dena Roberts
Emily Frazer
Paul Evans
Kelli Yates

Undergraduate Entry
American Nuclear Society
Student Design Competition

April 30, 2008

Faculty Advisor
Dr. M.L. Grossbeck

Nuclear Engineering Department
The University of Tennessee

Acknowledgements

We would like to extend our thanks to Dr. Ian McInnes for his lecture pertaining to dry cask storage methods, Mr. Benjamin Blalock for his lecture providing information on electronics, Dr. Roberto Benson for use of his resources and time spent in discussion, Dr. Paul Crilly and W.H. Andrews for electrical design. Additionally, we would like to thank Dr. Ronald Pevey for his assistance with shielding calculations. Also special thanks to Dr. Martin Grossbeck for equipment provision, design advice, and research that has greatly aided in this project.

Abstract

The introduction of nuclear power as a commercial industry included plans to temporarily store the depleted, spent fuel in large pools of water until sufficiently cooled for transport to reprocessing or permanent storage facilities. However, due to lack of government agreement, no permanent site for nuclear waste storage has been established, and the cost of reprocessing the fuel is not beneficial at this time. For every four fuel elements reprocessed approximately one fuel element is recovered that can be used for heat production in the core. Although the final destination for the waste has never been established, plants continue to produce power and spent fuel. With no other means of storage available, the spent fuel pools, which were intended for temporary storage, have become a permanent destination. Because enough space must be maintained to completely empty the core in the case of emergency and because a third of the fuel is depleted and removed from the reactor every 12 to 18 months, the spent fuel pools have been gradually filling up. At this point, with maximum pool capacity projected to be reached in the near future, it has become critical to find another solution for spent fuel storage if nuclear power is to survive.

One posed solution to this problem is the on-site storage of spent fuel in dry steel and concrete casks. These casks allow permanent storage of spent fuel after a cooling period of only 5 years in the pool. Because the dry storage casks are designed through use of conceptual understanding and computer modeling and due to safety concerns, the structures are constructed with conservative estimates. The methods of sealing the casks make conventional methods of measurement unusable; therefore, design of a system which could transmit internal environment conditions of the cask through the storage materials could provide measurements which would aid in more efficient cask design and decrease in cost.

This paper considers the components necessary to design a device to transmit critical information from the inside of a spent fuel dry storage cask to receiving equipment external to the cask. Due to available variations, the actual cask assembly is specified as a horizontal storage model. Measurement considerations include the use of pressure sensors and thermocouples to obtain temperature. In order to power the equipment various methods are considered with the conclusion that thermopiles are the most advantageous. For signal transmittance ultrasonic transducers are investigated and suggested. Although a special design of transducer would be the best candidate, this study concludes that the delay line transducer was the closest for this application. The various components used in the system design introduce separate shielding issues dependent on material properties.

Table of Contents

1.0 Background 1
2.0 Purpose 4
3.0 Design Basis 4
3.1 Cask Description 4
3.2 Storage Module Description 8
3.3 Design Criteria 10
4.0 Thermocouples 11
4.1 Thermocouple Theory 13
4.2 Thermocouple Properties 16
4.3 Addition System Components 18
5.0 Pressure Sensor 19
5.1 Types of Pressure Sensors 19
5.2 Pressure Sensor Selection 21
6.0 Power Supply 23
6.1 Types of Power Sources 23
6.1.1 Gamma Based Photovoltaic Cells 23
6.1.2 Nuclear Batteries 24
6.1.3 Thermopiles 24
6.2 Power Specification 25
7.0 Ultrasonic Data Transmission 29
7.1 Ultrasonic Transducer Theory 30
7.2 Types of Transducers and Components 36
7.2.1 Comparison of Transducers 36
7.2.2 Piezoelectric Material 38
7.2.3 Couplant Material 40
7.3 Testing Methods and Results 41
7.4 Radiation and Temperature Considerations 49
7.5 Summary of Recommendations 53
8.0 Radiation Shielding 54
8.1 Radiation Effects and Protection 57
8.2 Shielding Calculations and Results 58
9.0 External Data Transmission 69
10.0 System Design and Response 71
10.1 Design of Measurement System 71
10.2 System Experiment 73
11.0 Future Work 76
References 78
Appendix A: Standard Test From Provided by Olympus 81
Appendix B: Acoustic Properties of Materials 82
Appendix C: Near Field Lengths for 1020 carbon steel and 347 aus. Stainless steel 83
Appendix D: Values obtained using liquid silicone with 3/8 inch plate 83
Appendix E: Values obtained using petroleum jelly with 3/8 inch plate 85
Appendix F: Values obtained using magnesium hydroxide with 3/8 inch plate 86
Appendix G: Values obtained using liquid silicone with 6/8 inch plate 87
Appendix H: Voltage response due to addition of rough plates 88

Appendix I: Voltage response due to addition of smooth plates 88
Appendix J: Voltage response due to transducer offset 88
Appendix K: Pin Configuration of Multiplexer 89
Appendix L: Functional Block Diagram of Multiplexer 89
Appendix M: Functional Block Diagram of Operational Amplifer 89
Appendix N: Voltage-Controlled Oscillator Pin Configuration 90
Appendix O: Voltage-Controlled Oscillator Logic Diagram 90
Appendix P: SAS2 Sample Input Deck 91
Appendix Q: SAS1 Sample Input Deck 91

List of Figures

Figure 1.1 – Estimated spent fuel pool availability
Figure 1.2 – Vertical and horizontal dry storage systems
Figure 3.1 – Dry storage cask shell
Figure 3.2 – Basket assembly
Figure 3.3 – Complete DSC system
Figure 3.4 – Array of HSMs
Figure 3.5 – Passive cooling system in HSM
Figure 4.1 – Thermocouple tip styles
Figure 4.2 – Thermocouple circuit
Figure 4.3 – Voltage/temperature characteristics of various thermocouple types
Figure 4.4 – Thermocouple junction
Figure 6.1 – Thermopiles connected in series
Figure 6.2 – Ferro Tec Thermoelectric Module
Figure 7.1 – Illustration of Longitudinal and Shear Waves
Figure 7.2 – Wave Addition
Figure 7.3 – Fields produced by transducer
Figure 7.4 – Conventional transducer pulse versus various phased array pulses
Figure 7.5 – Beam spread angle
Figure 7.6 – Aperture Size versus Beam Steering
Figure 7.7 – Electromagnetic Acoustic Transducer
Figure 7.8 – Cross-sectional view of tangential field EMAT
Figure 7.9 – Contact Transducer Dimensions
Figure 7.10 – Dual Element Transducers
Figure 7.11 – Delay Line Transducer
Figure 7.12 – Transducer Components
Figure 7.13 – Frequency vs Near Field Length
Figure 7.14 – Experimental setup with 3/8 inch stainless steel plate
Figure 7.15 – Voltage vs Frequency for 9.525 mm plate & Liquid Silicone Couplant
Figure 7.16 – Voltage gain (-dB) vs Frequency for 9.525 mm plate & Liquid Silicone Couplant
Figure 7.17 – Voltage vs Frequency for 9.525 mm plate & Petroleum Jelly Couplant
Figure 7.18 – Voltage gain (-dB) vs Frequency for 9.525mm plate & Petroleum Jelly Couplant
Figure 7.19 – Voltage vs Frequency for 9.525 mm & $Mg(OH)_2$ Couplant
Figure 7.20 – Voltage gain (-dB) vs Frequency for 9.525mm & $Mg(OH)_2$ Couplant
Figure 7.21 – Comparison of voltage response versus frequency for couplants on 9.525 mm plate
Figure 7.22 – Voltage vs Frequency for 19.05 mm & Liquid Silicone Couplant
Figure 7.23 – Voltage gain (-dB) vs Frequency for 19.05 mm & Liquid Silicone Couplant
Figure 7.24 – Voltage response vs Plate thickness (rough plate with rough plate addition)
Figure 7.25 – Voltage response vs Plat thickness (smooth plate with rough plate addition)
Figure 7.26 – Voltage response vs Transducer-to-transducer offset distance
Figure 7.27 – Voltage gain (-dB) vs Transducer-to-transducer offset distance

Figure 7.28 – Melting temperatures from polymer samples versus absorbed radiation
Figure 7.29 – Melting temperature and heat of melting for polymers versus absorbed dose
Figure 7.30 – Crosslinking percentage in polymer as a function of absorbed dose by gamma irradiation
Figure 8.1 – Total decay heat versus cooling time for NUHOMS 24PL cask
Figure 8.2 – Gamma decay heat versus cooling time for NUHOMS 24PL cask
Figure 8.3 – Actinide and fission fragment activity versus cooling time for NUHOMS 24PL cask
Figure 8.4 – Neutron source term versus assembly power
Figure 8.5 – Photon source term versus assembly power
Figure 8.6 – Neutron source term versus cooling time
Figure 8.7 – Gamma source term versus cooling time
Figure 8.8 – Unmodified cask design SAS1 model
Figure 8.9 – SAS1 model of modified shield design
Figure 8.10 – Log of gamma dose rate (R/hr) versus shield depth in the top of a NUHOMS 24PL cask
Figure 8.11 – Neutron dose rate (R/hr) versus shield depth in the top of a NUHOMS 24PL cask
Figure 8.12 – Dose rate (R/hr) versus cooling time in electronics region of modified shield design in a NUHOMS 24PL cask
Figure 8.13 – Outside cask dose rates versus cooling time
Figure 10.1 – Layout of System Design
Figure 10.2 – Layout of Experimental Setup
Figure 10.3 – Experimental Circuit Diagram
Figure 10.4 – Frequency versus Thermocouple Temperature

List of Tables

Table 4.1 – Comparison of Sheath Materials
Table 4.2 – Standard Thermocouple Types
Table 7.1 – Couplant Types and Characteristics
Table 7.2 – Calculated values for 1020 carbon steel and 347 austenitic stainless steel
Table 8.1 – B & W 15x15 fuel assembly specifications
Table 8.2 – Source term parametric study results
Table 8.3 – Source terms versus cooling time results
Table 8.4 – Area-averaged accumulated dose outside of cask
Table 10.1 – Frequency produced by VCO versus temperature of thermocouple

1 Background

In commercial American power reactors, the fuel is composed of low-enriched uranium (3-5% ^{235}U) pellets, in the form of uranium dioxide, that are loaded into a Zircaloy tube to create a fuel rod. These rods are formed into fuel assemblies with geometries ranging from 14x14 to 17x17. Each assembly has coolant channels and guide tubes in the place of some fuel rods and the number and location of each varies by manufacturer.

At the end of each cycle (12-18 months) at a nuclear power plant, approximately 1/3 of the fuel assemblies in the core are replaced with new ones. The ones that are removed are known as spent fuel or used fuel. Since the United States currently does not reprocess its used nuclear fuel, the spent fuel assemblies are moved from the reactor core to an on-site storage pool. Although the nuclear fuel is depleted enough to warrant replacement, it still generates large amounts of heat and radiation for many years and thus must be stored in a facility that shields the radiation and allows for proper heat removal. Storage pools shield the radiation by placing the fuel assemblies under more than 20 feet of water and are actively cooled to maintain adequate heat removal.

These spent fuel pools, however, were not meant for permanent storage of radioactive material. When most commercial power plants were built in the U.S., the plan was to keep spent fuel in on-site storage pools until it was cool enough to transport to a reprocessing facility or permanent waste disposal site. Under the Carter administration, all funding for reprocessing facilities were halted and the proposed geological repository at Yucca Mountain is still politically controversial. While a permanent solution for used fuel is argued in the political arena, the spent fuel pools that were meant for temporary storage continue to fill up. According to

Department of Energy estimates shown in Figure 1.1, 80% of spent fuel pool storage space is already full in the United States and that it will reach carrying capacity by the year 2014.

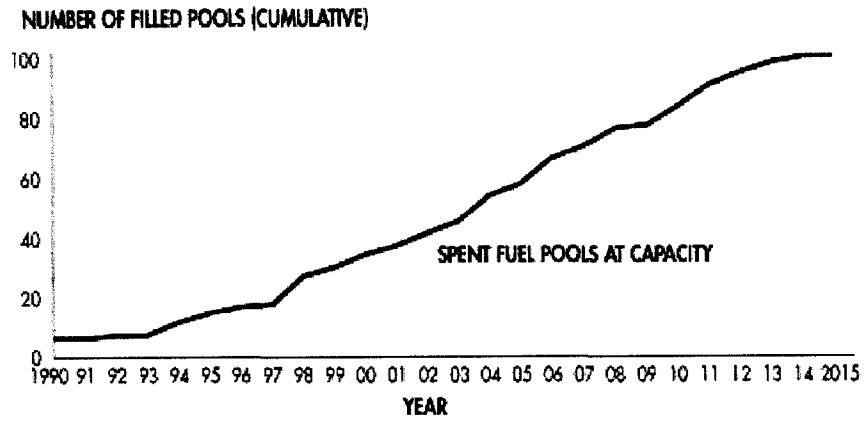

Note: All operating nuclear power reactors are storing used fuel under NRC license in spent fuel pools. Some operating nuclear reactors are using dry cask storage. Information is based on loss of full-core reserve in the spent fuel pools.

Source: Energy Resources International and DOE/RW-0431 - Revision 1

Figure 1.1 Estimated spent fuel pool availability

In response to the dwindling free space in spent fuel pools, new storage solutions were sought. One of these solutions is the utilization of independent spent fuel storage installations (ISFSI), which are wet or dry storage facilities other than spent fuel pools and can be either at the reactor site or at a new location. One of the most popular forms of ISFSI is the dry cask on-site storage system, which utilizes large metal and concrete vessels to house spent fuel assemblies that have cooled at least 5 years in a spent fuel pool. These systems generally consist of a steel vessel to hold the assemblies and a concrete and steel housing block to shield the vessel. For casks that are stored vertically, the concrete structure is typically a cylinder that is placed around the steel vessel and for horizontally stored casks, the steel vessel is usually loaded into a concrete housing that is the size of a single car garage. Both types are illustrated in Figure 1.2.

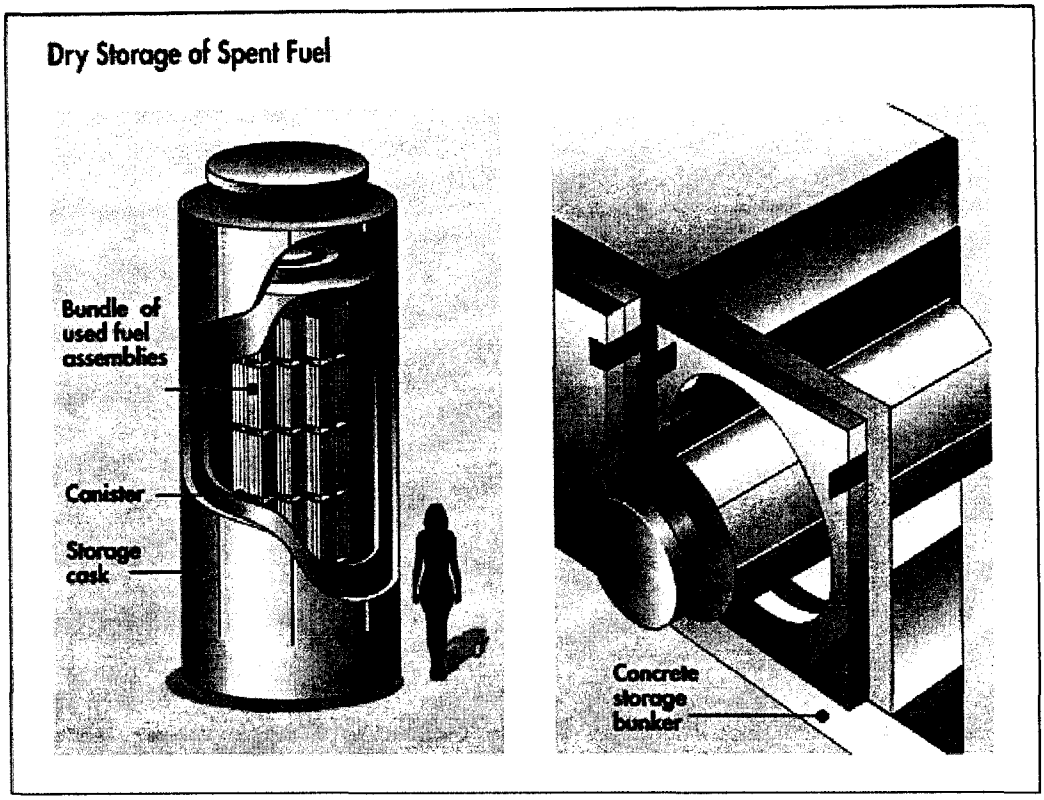

Figure 1.2 Vertical and horizontal dry storage systems

The first of these dry cask storage systems received general licensing by the NRC in 1990 and since then, 46 sites across the U.S. have adopted the system. In the almost 20 years since its usage began, there have been no radiation leaks, contaminations, or significant accidents involving dry cask storage methods. Since they are designed with the same criteria as power plant facilities, the storage housings are designed to withstand tornados, hurricanes, earthquakes, floods, projectiles, and other disasters without releasing any of their contents to the environment.[1]

2 Purpose

Because of the stringent design criteria applied to the dry cask storage facilities to prevent radiation leakage, the cask pressure boundaries are redundantly sealed and no holes are allowed to penetrate these boundaries. This means that conventional methods used to measure critical data in systems such a nuclear reactor cannot be used because they transmit their information from the core through wires. Therefore, casks are currently designed based on very conservative computer simulations to ensure subcriticality, proper heat removal, and low internal pressure. If one were able to measure critical information such as temperature and pressure from inside the cask and transmit it through the vessel without breaking the pressure boundary, one would be able to have a more accurate picture of what really occurs inside the cask during storage. This could eliminate the need for unnecessary conservatism in cask design, which would lead to improved storage efficiency and reduction in the overall cost to utilities in implementing dry cask storage systems. Therefore, our team set out to design a system that would measure temperature and pressure inside a spent fuel storage cask and transmit that information through the pressure vessel without breaking the pressure boundary. Since the dry storage casks are licensed for 100 year operating periods, our system also has to remain operational for several decades without maintenance.

3 Design Basis

3.1 Cask Description

The most popular dry storage system in the United States is the NUHOMS system from Transnuclear Inc. The NUHOMS storage system is comprised of horizontal storage modules and

dry storage casks. There are currently 325 of the NUHOMS casks in operation and over 140 more have been ordered. Because of its popularity, this system was chosen as our design basis.

Transnuclear offers many different types of casks based on fuel type and storage needs. Each cask can store anywhere from 7 to 61 fuel assemblies and is designed for PWR, BWR, or VVER spent fuel. The casks are also designed based on the maximum burnup of the fuel to be stored and can accommodate ranges between 40,000 and 60,000 MWd/MTU.[2] The NUHOMS 24P, a cask for 24 PWR regular burnup fuel assemblies, was chosen as our design basis because a majority of power reactors in the U.S. are PWRs and because the 24 assembly regular burnup model is the most popular option.

The NUHOMS Dry Shielded Canister (DSC) is a stainless steel cylindrical shell with stainless steel top and bottom double seal welded cover plates. This shell comprises the pressure boundary of the cask. Carbon steel or lead encased in carbon steel shield plugs are used at both ends of the cask and held in place within the pressure boundary shell with supporting rings that are attached to the inside of the shell. The area between the shield plugs is where the fuel assemblies are stored. The assemblies are loaded into a basket assembly with slots for each assembly. Each cask has stainless steel guide sleeves that encase the fuel assemblies and eight stainless steel spacer discs. Spacer discs are used to maintain cross sectional spacing and four support rods are used to hold the spacer disc in place. The cask, basket assembly, and complete DSC system are shown in Figures 3.1-3.3 below.

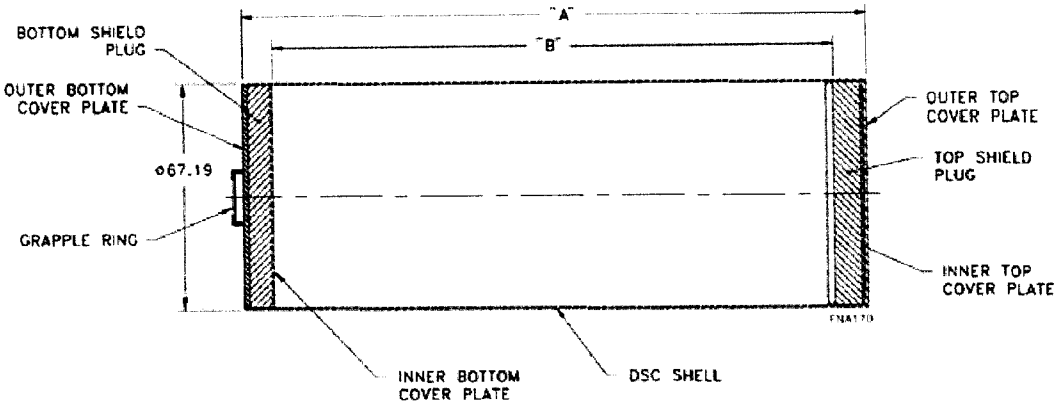

Figure 3.1 Dry storage cask shell (units in inches)

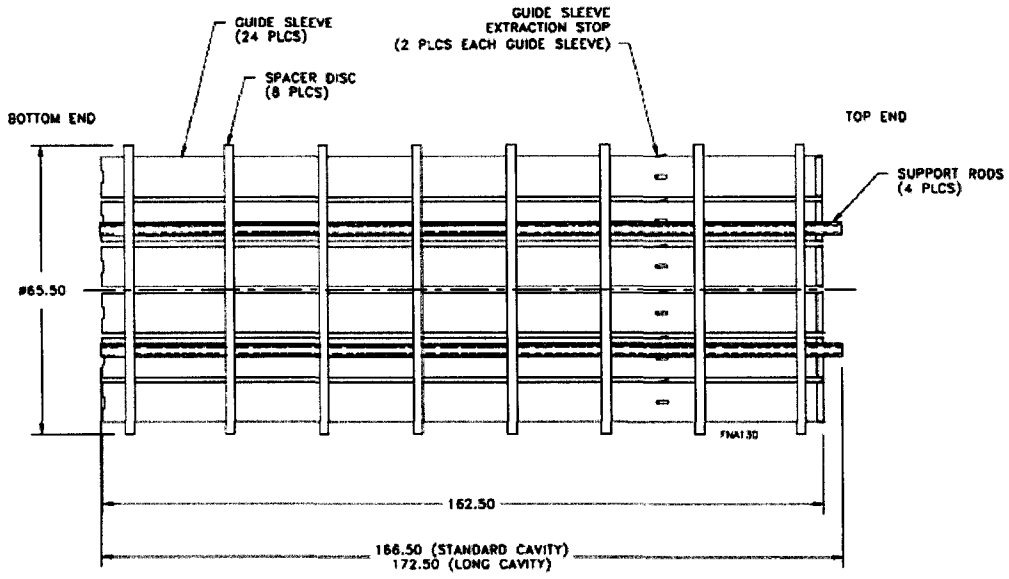

Figure 3.2 Basket assembly (units in inches)

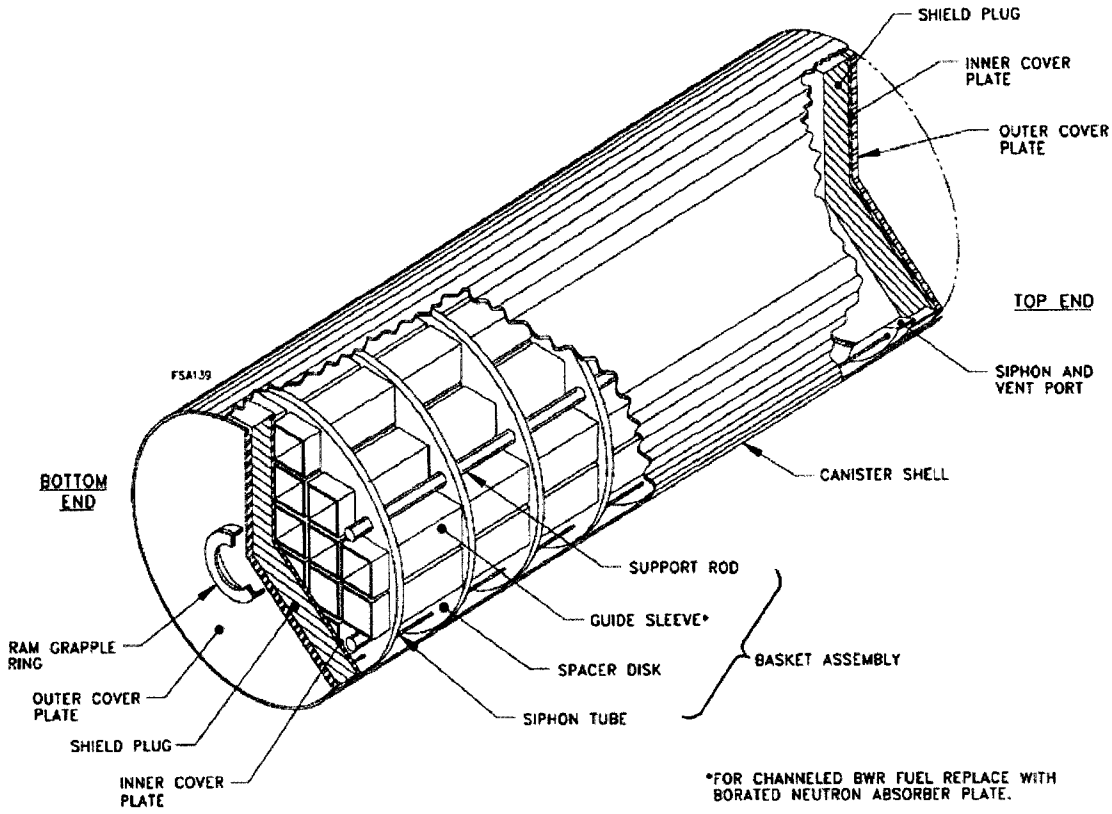

Figure 3.3 Complete DSC system

The bottom shield plug is installed prior to fuel loading. To load spent fuel into the cask, the DSC is lowered into the spent fuel pool and flooded with water. The fuel assemblies are moved individually into the cask while still under water. Once all of the assemblies are loaded, the top shield plug is lowered onto the support ring and the water inside the cask is forced out by pumping compressed air, nitrogen, or helium into the vessel. Once all of the water is out, the remaining moisture is removed through vacuum drying, and the inner and outer cover plates are welded in place. The DSC is then placed in a concrete and steel transport cask and transported to the Horizontal Storage Module (HSM) via trailer.[3]

3.2 Storage Module Description

The Horizontal Storage Module is a reinforced concrete housing that provides additional radiation shielding and environmental protection for the cask. The side walls are 1.5 feet thick and the rear walls are 2 feet thick. The HSM contains four shielded air vents at the bottom of the side walls and four shielded exit vents near the top of the housing. Cool air enters the HSM at the bottom, envelopes the cask, and the heated air is removed through the top exit vents, thus providing a passive decay heat removal system for long term storage.

The DSC is loaded through a steel and concrete door assembly that is approximately 2 feet thick with a ½ inch steel liner on its inner side. The DSC is held above the floor with support rails. These are made of structural steel and are anchored to the HSM floor, side walls, and front wall opening.[3] An array of Horizontal Storage Modules and the passive cooling system are illustrated in Figures 3.4 and 3.5 below.

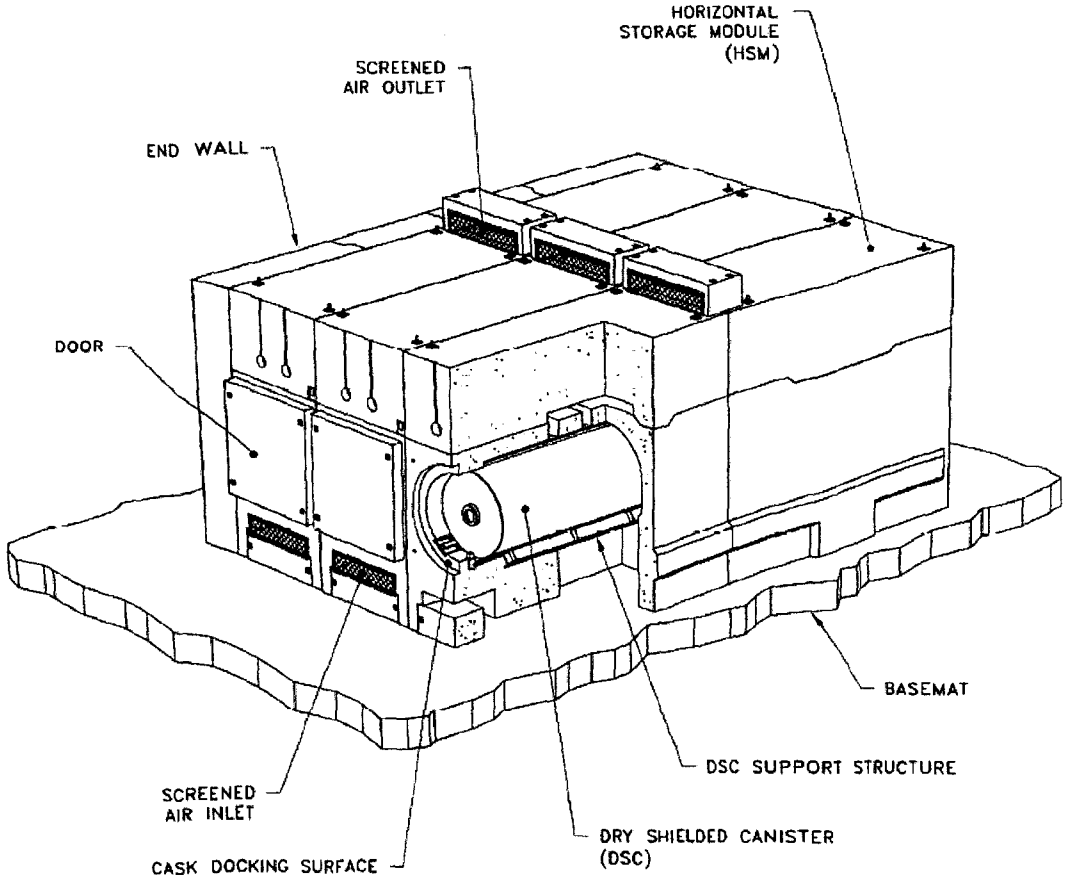

Figure 3.4 Array of HSMs

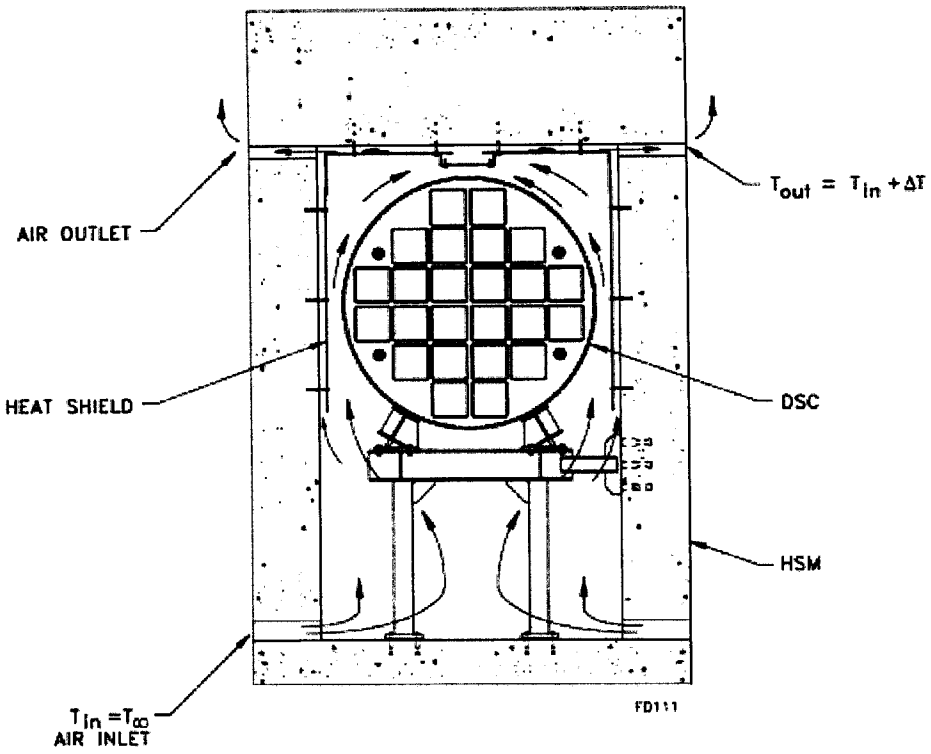

Figure 3.5 Passive cooling system in HSM

3.3 Design Criteria

The purpose of the system will be to monitor the internal conditions of the cask and transmit relevant information through the cask wall where it can be recorded and analyzed. The most important internal parameters are temperature and pressure. Temperature is important to monitor because fluctuations can indicate failed fuel rods, ventilation problems, and criticality excursions. Pressure measurements can indicate failed fuel rods and pressure boundary leaks.

There are several constraints in designing this system. First, the primary pressure boundary cannot be broken. This means that the information measured by pressure and temperature sensors must be transmitted wirelessly through the cask wall. This also means that

the measurement and transmission components have to be internally powered since no wires can connect the components to an outside power source. Second, the electronics must be able to withstand the extreme environment inside of the storage vessel. The individual system components must be able to withstand the high temperatures, which peak around 400°C, as well as gamma and neutron radiation from the used fuel. Radiation-hardened electronics can generally withstand 1 MR of radiation, which is our upper limit on allowed accumulated dose over the lifetime of the system (40 years or more). Additionally, modifications to the cask must be kept to a minimum to ensure that implementing this design will not be prohibitively expensive.

4 Thermocouples

A thermocouple is a sensor that measures temperature. It consists of two different types of metals, joined together at one end. When the junction of the two metals is heated or cooled, a voltage is created that can be correlated to temperature. There are many different kinds of thermocouples that cover a wide range of temperatures and are used in different environments based on the requirements of the project. Some of the common ways to figure out what the best thermocouple is for the specific project at hand is the temperature range that is needing to be measured, the chemical resistance of the thermocouple or sheath material, its ability to stand up to abrasion and vibration as well as the installation requirement or in our case the space restrictions. Most of these elements need to be taken into consideration when choosing a thermocouple.

Another aspect of choosing a thermocouple is the type of junction: whether it should be grounded, ungrounded, or exposed. A grounded thermocouple is where the thermocouple wires

are attached directly to the inside of the probe wall and there is good heat transfer between the outside of the probe through the probe wall to the thermocouple junction. The response time is a little slower than that of the exposed junction thermocouple but also has the added benefits of being able to work in wet, corrosive, and pressurized environments. The exposed has the best response time but is limited to non-harsh environments that are not pressurized. The reason that the exposed junction thermocouple cannot withstand a pressurized environment is because it is not protected by the sheath material like the grounded and ungrounded thermocouple junctions. Finally, the ungrounded is where the thermocouple junction is detached from the probe wall. This type has the slowest response time but it offers an electrical insulation (Figure 4.1). One of the final things to take into consideration is the type of sheath material that will be used for the thermocouple because the sheath material may not be able to withstand the full temperature range of the thermocouple. A sheath is the part of the thermocouple that protects the insulation and wires from physical damage, contamination and the environment, all of which affect the service life and cost. As there isn't any one particular sheath material that is appropriate for all conditions, a couple of materials that are frequently used are stainless steel 304 and Inconel 600.

Figure 4.1 Thermocouple tip styles

Table 4.1 Comparison of Sheath Materials

Material	Maximum Temperature	Application Atmosphere			
		Oxidizing	Hydrogen	Vacuum	Inert
304 SS	900°C (1650°F)	Very Good	Good	Very Good	Very Good
Inconel 600	1148°C (2100°F)	Very Good	Good	Very Good	Very Good

4.1 Thermocouple Theory

The driving force behind the thermocouple is the Seebeck effect, which is the conversion of heat directly into electricity. This is done by joining the ends of two strips of dissimilar metals and creating a closed loop. When the two junctions of the metals are at different temperatures, a voltage arises that is proportional to the temperature difference between the junctions. That difference increases with temperature, and can typically be between 1 and 70 micro-volts per degree Celsius (μV/°C) for the modern range of available metal combinations.

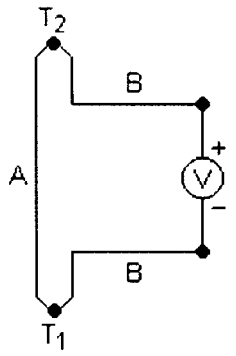

Figure 4.2 Thermocouple circuit

$$V = \int_{T_1}^{T_2} \left(S_B(T) - S_A(T)\right) dT \tag{4.1}$$

The above formula describes the relationship between the voltage and temperature difference. S_A and S_B are the Seebeck coefficients of metals A and B as a function of temperature, and T_1 and T_2 are the temperatures of the two junctions[5]. The Seebeck coefficients are non-linear as a function of temperature, and depend on the conductor's absolute temperature, material, and molecular structure. If the Seebeck coefficients are effectively constant for the measured temperature range, the approximated formula is:

$$V = (S_B - S_A) \cdot (T_2 - T_1) \tag{4.2}$$

Figure 4.3 below shows the voltage- temperature spectrum of the most popular types of thermocouples[4]. It shows that there is a near linear correlation between temperature and voltage. Also below in Table 4.2 lists the different types of thermocouples and the materials that they are made of.

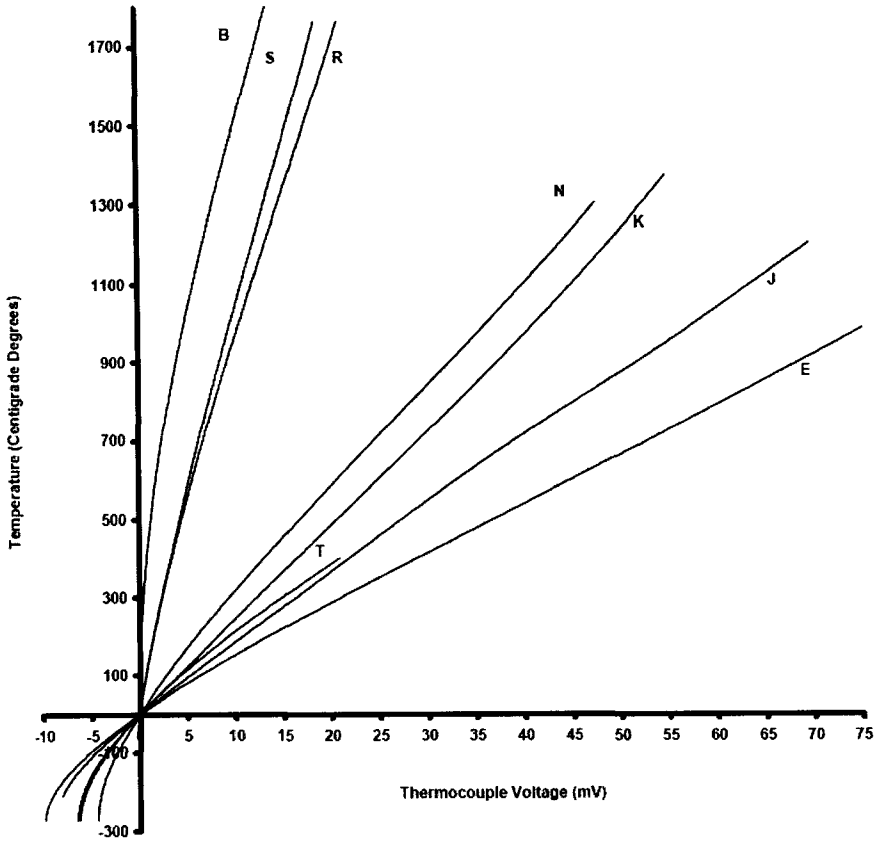

Figure 4.3 Voltage/temperature characteristics of various thermocouple types

Table 4.2 Standard Thermocouple Types

Type	Materials*	Typical Range °C
T [1, 2]	Copper (Cu) vs Constantan	-270 to 400
J [1, 3]	Iron (Fe) vs Constantan	-210 to 1200
K	Chromel vs Alumel	-270 to 1370
E	Chromel vs Constantan	-270 to 1000
S	(Pt-10%Rh) vs Pt	-50 to 1768
B	(Pt-13% Rh) vs (Pt-6% Rh)	0 to 1820
R	(Pt-13%Rh) vs Pt	-50 to 1768
N	(Ni-Cr-Si) vs (Ni-Si-Mg)	-270 to 1300

The materials that the above thermocouples consist of are as follows[5]:

*Material Definitions:

- Constantan, alloy of Nickel (Ni) – Copper (Cu)
- Chromel, alloy of Nickel (Ni) – Chromium (Cr)
- Alumel, alloy of Nickel (Ni) – Aluminum (Al)
- Magnesium (Mg), a base element
- Platinium (Pt), a base element
- Nickel (Ni), a base element
- Silicon (Si), a abase element
- Chromium (Cr), a base element
- Iron (Fe), a base element
- Rhodium (Rh), a base element

4.2 Thermocouple Properties

Aside from the specified accuracies of the data acquisition system, most thermocouple thermometry measurement errors can be traced to one of these primary sources[5]:

1. Poor junction connection
2. Decalibration of thermocouple wire
3. Shunt impedance and galvanic action
4. Thermal shunting
5. Noise and leakage currents
6. Thermocouple specifications
7. Documentation

Of the problems that face thermocouples there are several that we have to take into consideration while doing this project and they are decalibration of the thermocouple wires, and shunt impedance.

Decalibration is a serious condition because it can result in an erroneous temperature reading that appears to be correct. Decalibration describes the process of unintentionally altering

the physical makeup of the thermocouple wire so that it no longer conforms to the NBS polynomial within specified limits. Decalibration can result from diffusion of atmospheric particles into the metal caused by temperature extremes. It can be caused by high temperature annealing or by cold-working the metal, an effect that can occur when the wire is drawn through a conduit or strained by rough handling or vibration. Annealing can occur within a section of wire that is subjected to a high temperature.

Thermocouple wire obviously can't be manufactured perfectly; there will be some defects which will cause output voltage errors. These inconsistencies can be especially troublesome if they occur in a region of steep temperature gradient. Since the location of an imperfection is undeterminable within a wire, the best alternative is to avoid creating a steep gradient. Gradients can be reduced by using metallic sleeving or by careful placement of the thermocouple wire.

To deal with the extreme temperatures a well insulated wire should be used that can withstand the high temperatures for the duration of the project. A specific wire, for example, is manufactured by Ceramawire[6]. It is a high temperature magnet wire insulated with a fully cured vitreous enamel film, which is firmly bonded to the wire conductor; the insulation assumes the same flexibility and temperature coefficient of the base wire. Tests by Oak Ridge National Lab show that it has a high resistance to radiation making it suitable for nuclear applications. This wire has also proven capable of withstanding temperatures of 1000° F under continuous operation[6]. However tests would need to be conducted to make sure that the wire would be able to relay accurate data after having been under such extreme conditions for thirty plus years.

Based on the requirements that will be put on the thermocouple, the best type of thermocouple to use would be a, k type chromel/alumel thermocouple that is grounded with

inconel 600 for the sheath material. The thermocouple is a high temperature inconel overbraided ceramic fiber insulated thermocouple style #1 manufactured by OMEGA Engineering, INC. One Omega Drive Stamford, Connecticut 06907

4.3 Additional System Components

To go along with the thermocouple a thermocouple amplifier with cold junction compensation will be needed. Cold junction compensation (CJC) is when the reference junction is not zero °C which is what standard thermocouple look-up tables are referenced to. As a result, the actual measured voltage must be adjusted so that it appears as referenced to zero °C[31]. The amplifier portion is needed in order to get enough of a signal out of the cask to analyze the output voltage. The thermocouple amplifier that was chosen for this project is the monolithic thermocouple amplifier with cold junction compensation AD595 from Analog Devices Inc. One Technology Way, P.O. Box 9106, Norwood, MA

Another electronic device that will be used in conjunction with the thermocouple amplifier is a multiplexer that allows readings to be obtained from multiply thermocouples without having to have an amplifier with each thermocouple. The multiplexer cycles through multiple channels and gives a reading that can then be amplified and sent out though the transducer. The multiplexer that was chosen, works well in conjunction with the AD595 amplifier, is the ADG506A/ADG507A from Analog Devices Inc. [30] One Technology Way, P.O. Box 9106, Norwood, MA. The 506 model has sixteen inputs to a common output and the 507 model has eight inputs to a common output. Either model is feasible, but due to model specifics the number of inputs required has not been determined at this time.

The final piece of electronic equipment that will be used is the voltage controlled oscillator. The voltage controlled oscillator (VCO) is an electronic oscillator designed to be controlled in oscillation frequency by a voltage input[32]. The frequency of oscillation is varied by the applied DC voltage. This is going to be used to vary the voltage that is being generated by the thermocouple in order to determine the temperature inside the cask at a given point. The VCO that will be used for this project is from the SN54LS624 thur SN54LS629 series manufactured by Texas Instruments PO BOX 655303 Dallas, TX.

5 Pressure Sensor

Helium is used as a cover gas in the spent fuel storage cask to easily remove decay heat and to keep the integrity of the contents. Monitoring the pressure in the cask will allow the owner of the cask to know if the cover gas has changed any. Because the design is supposed to last for forty years, this knowledge will help the owners and the Nuclear Regulatory Commission know the integrity of design. Knowing that the fill gas is still there will help prove that safety of the cask is not interrupted and no major events have occurred with the fuel being stored. This knowledge will be quite useful in extending the life of the cask.[3]

5.1 Types of Pressure Sensors

Several ways exist for measuring pressure and are currently in use in industry. When looking for a sensor to measure the pressure inside the cask, it is necessary to study the different types and make a decision based on this knowledge. The study begins with the types of mechanical methods available for measuring pressure. Manometers, bellows, diaphragms, and

bourdon tubes all represent mechanical ways to observe pressure. Manometers are quite large and involve a u-shaped tube containing liquid to measure pressure. The size and containment of liquid make the manometer an option we cannot use. Bourdon tubes are hook shaped and involve a large change in form. This large displacement is not very useful in electromechanical devices like this project would call for. Diaphragms allow small movements with pressure and are better for sensors.

In order to be useful, this mechanical displacement has to be converted into an electrical signal. This is now what one would call an electromechanical pressure sensor or a pressure transducer. Gauge, absolute, differential, and sealed are all types of reference options for a pressure sensor. Ways to convert the mechanical energy to an electrical signal are use of strain gauges, variable capacitance, and piezoelectric devices.**Error! Reference source not found.**

The strain gauge is attached to the deformation part of the pressure sensor. The material for strain gauges undergoes resistance change when the gauge is compressed or stretched. The resistance change is proportional to the change in length. This change in resistance can be modeled using Equations 5.1 and 5.2:

$$R = \rho L/A \qquad \textbf{(5.1)}$$

$$\Delta R/R = GF \cdot \Delta L/L \qquad \textbf{(5.2)}$$

R is the resistance, L is the length, A is the cross-sectional area, GF is the gauge factor, and ρ is resistivity. This resistance change determines the electrical output of the system. In some cases the gauges may be diffused onto the diaphragm using micro assembly. This allows for the best

placement of the strain gauges, removal of the bonding agent properties, increases sensitivity, and allows the gauge to be smaller.[7]

Capacitance transducers work differently. One plate of the capacitor is the diaphragm. When the pressure changes, the distance between the two plates changes. This change in the capacitance is then used to either vary an oscillator's frequency or is detected by a bridge circuit. This method has good stability and repeatability.

Piezoelectric transducers use layers of piezoelectric crystals to change motion of a mechanical method into an electrical signal. The crystals used in this method create an electrical charge when they are strained. While this method does not require an outside excitation, they do require some signal conditioning such as special cables and amplifiers. Because they create a charge when there is a change in the strain, they are not good candidates for static measurements.[8]

5.2 Pressure Sensor Selection

After looking at the types of transducers available for pressure measurements, the diaphragm and strain gages present the best option for our design. It is necessary to find one that will fit our specific needs. Size, temperature, pressure range, radiation hardness, excitation voltage, output are all factors that must be kept in mind when deciding upon a transducer for our system. The instrument should be able to handle relatively low pressures, and it should withstand high operating temperatures. Excitation voltage should be low in order to reduce the amount of power required inside the cask. Omega's PX1009 meets most of the requirements. This particular pressure transducer uses a stainless steel diaphragm with a sputter-deposited strain gauge for maximum performance. It can withstand temperatures from -65 to 650 degrees

Fahrenheit. With dimensions of 2.4 inches by 1.01 inches, space is available inside the cask for the instrument to be placed. This model is also offered in several pressure ranges. Based on the calculations performed by the cask manufacturers, the pressure range 0 to 250 psi should cover the range of possible pressure under normal and accident conditions. This particular transducer requires 10 volts excitation. This is higher than the voltage required to operate the other electronics but can be supplied using the same method of thermopiles. The voltage can then be regulated using a voltage control regulator. The output from the transducer is in the millivolt range. When added to the temperature measurement system in the cask, it is attached to the amplifier. Data from this amplified voltage can then be attached to the appropriate electronics and transmitted out of the cask. This particular pressure transducer does not list a radiation dose limit. The pressure sensor is incased in stainless steel. Stainless steel is a shielding material. This would minimize the amount of radiation entering the pressure transducer. Inside the incasing, the diaphragm is made of stainless steel with strain gauges of metal also.[9]

Problems with this pressure transducer might occur if temperature increases to a point higher than 650 degrees Fahrenheit. However, based on the manufacturer performed calculations, such temperatures will not be reached at places where the transducer may be placed. If pressure changes frequently over the time, the metal diaphragm may lose its bending characteristics. However, if pressure changes frequently in cask over time, this would mean the transducer has found a problem which would be the reason for initially monitoring the cask.[3]

6 Power Supply

The device requires power to run the electronics and output the signal from the transducer. Inside the cask the harsh environment and space limitations make selecting a good power source difficult. There are three basic ideas of power generation for this type of application considering the limitations and requirements: photovoltaic cells, a nuclear battery, and a thermopile or thermoelectric generator. All three devices could work, however the use of thermopiles and the heat generated from the spent fuel is believed to be best choice for the design because of their durability and effectiveness.

6.1 Types of Power Sources

6.1.1 Photovoltaic Cells

Photovoltaic cell technology is continuing to develop and has potential for powering the device. These cells use the gamma particles from the decay of spent fuel to produce electrical energy. Due to space restrictions inside spent fuel casks, photovoltaic cells have the benefit of compact size. Another benefit of using photovoltaic cell technology is the large amount of voltage generated. However, the amount of power produced will not remain constant because the gamma flux from the spent fuel, which is initially quite high, will slowly decrease over time.

The primary concern with this type of application is the extremely large amount of radiation damage that would occur during the length of time the device is intended to survive. Over time the voltage output and efficiency will decrease due to the overwhelming amount of radiation, especially after twenty years. The space industry is still working on developments for radiation hardened photovoltaic cells which can remain efficient for decades. Another consideration is the extreme temperatures that the photovoltaic cells are subjected to during the

loading process. Further developments from this in photovoltaic cell technology might make this option a better choice in the future but as of now they seem to be undesirable for this application.

6.1.2 Nuclear Batteries

Nuclear batteries are reshaping the potential of the battery market. They use radiation from radioactive decay to produce energy and appear to be a very reasonable option considering lifetime and environment for this type of power application. Nuclear batteries also deliver power more consistently. However, placement of a nuclear battery in a spent fuel storage cask introduces another radioactive source into the cask environment. Also, nuclear batteries are relatively expensive in comparison to power received. However, they should be considered as a possible backup option for power production.

6.1.3 Thermopiles

Thermopiles or thermoelectric generators seem like a better option because of their reasonable cost and high tolerance for radiation. Thermopiles utilize the heat from the spent fuel to power the electronics. The main disadvantages of using thermopiles have to do with placement and the large number that is required to achieve a voltage high enough to drive the transducer. Thermopiles, unlike the voltaic cells, emit high amperage but low voltage. However a thermopile can also be modified to fit any particular casks configuration.

Thermopiles are made by linking multiple thermocouples together in series in order to increase the power output. Multiple thermopiles can then be put in parallel in order to further increase the output. Thermopiles use environmental heat energy gradients across two different

metals to obtain a desired power through the Seebeck effect. Figure 6.1 shows an example of how the Seebeck effect works when thermopiles are connected in series.

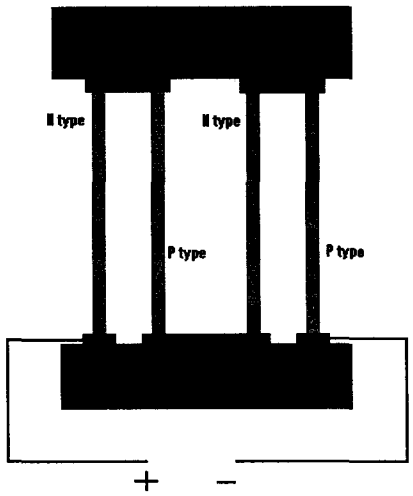

Figure 6.1 Thermopiles connected in series

The N type and P type semiconductors create an opposite charge from the temperature gradient. A thermopile can be made rather small and can be specifically designed for a specific cask.

6.2 Power Specification

In designing a thermopile for the cask, the most ideal solution would be to have the cold junction at the bottom side and along the edge of the cask while the hot junction is in the center of the spent fuel. The hot junction could be placed in the center of the fuel by attaching them to steel rods, which could then be lowered into the fuel assemblies through their guide tubes. This would require very thin diameter thermopiles but this will most likely lead the greatest amount of power with the least complexity.

Another design could use many thermopiles already available in the market today along the edge of the cask in order to create the necessary power. This would work but would require a lot of them to be used given their size and available placement in the cask. If the temperature difference is increased due to the use of heat sinks this idea becomes more feasible.

The power generated from a thermopile can be calculated using the following formulas:

$$V = S \times \Delta T \tag{6.1}$$

$$I = \frac{S \times \Delta T}{R_c + R_L} \tag{6.2}$$

$$P = \frac{(S \times \Delta T)^2}{4xR_M} \tag{6.3}$$

Here, V is voltage, S is the Seebeck coefficient in V/K, T is the absolute temperature, I is the current, R_c is average internal resistance, R_L is the load resistance, P is power, and R_M is the resistance of the pile.

The first proposed design of a thermopile power source for the device is to create thermopiles for a specific fuel assembly type. Therefore, the size of the thermopiles could be calculated based on the size of the guide tubes. Then multiple wires would be run from the center of the fuel to the cold junction in a corner of the cask and then be connected in series. This will allow for a large temperature gradient but will require custom designed thermopiles. This type of design will require very thin wire but will yield more power with fewer thermopiles than the alternative design.

In order to show that the use of a thermopile power supply is feasible, several calculations need to be performed to obtain the estimated size of the thermopile that is needed. It

is assumed that a 10 volt and 1 ampere power supply is required to the run the device. The approximate temperature near the center of the fuel region of the cask is 588.2 K (600°F) and 423.2°K (300°F) at the lower edge of the cask.[3]

$$\Delta T = T_H - T_C = 588.2 - 423.2 = 156K \qquad \textbf{(6.4)}$$

The thermopile technical references for a 127-couple high power thermoelectric module model 9500/127/120B are used for this calculation.[25]

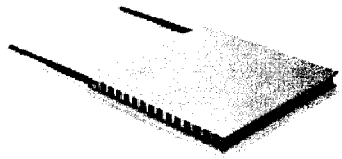

Figure 6.2 Ferro Tec Thermoelectric Module

This particular thermoelectric module would not fit the current design due to its size and shape but is properties should give a good estimate to the type of values one could expect.

$$\text{S(module)} = S_m = .04882$$

$$\text{R(module)} = R_m = 5.6801$$

Using Equation 6.3 the power from one thermoelectric module unit is:

$$P_M = \frac{(S_M \times \Delta T)^2}{4xR_M} = \frac{(.04882 \times 156)^2}{4x5.6801} = 2.784\text{watts}$$

The power requirement is equal to:

$$P = IR = 10 \times 1 = 10 \text{ watts}$$

Therefore the number of modules required:

$$N_m = \frac{10}{2.784} = 3.59 \Rightarrow 4 \text{ modules}$$

This shows that the concept is reasonable if properties of this type of thermopile can be obtained from the proposed thermopile design.

The second design is to use several of these Ferro Tec 127 thermoelectric modules together to create power, but they must be placed near the walls of the cask. Heat exchangers will go from the center of the cask to one side of the thermoelectric module to create the hot junction. The cold junction will be attached to the cask wall. The temperature difference will not nearly be as great as between the center of the core and the cask wall but this could still provide satisfactory power.

In order to show that this thermopile power supply design could be used, calculations similar to those performed for the first design will be repeated for the second design. Given the thermopile location along the sidewall of the cask, a conservative estimate for the temperature at the hot junction is 408.2 K (275 °F) and 377.6 K (220 °F).[2] Using Equation 6.4 again:

$$\Delta T = T_H - T_C = 408.2 - 377.6 = 30.6K$$

Using Equation 6.3 the power from one thermoelectric module unit is:

$$P_M = \frac{(S_M \times \Delta T)^2}{4xR_M} = \frac{(.04882 \times 156)^2}{4x5.6801} = 0.1333\text{watts}$$

Therefore the number of modules required:

$$N_m = \frac{10}{0.1333} = 75.02 \Rightarrow 76 \text{ modules}$$

While the number of modules for this estimation is high, these modules are very small at 3.97cm x 3.97cm x 3.45mm. The purpose of this project is to show that this type of device is feasible and from these power calculations this appears to be true for either thermopile design. The first design uses a fewer number thermopiles and is the recommended design but both designs are viable options.

7 Ultrasonic Data Transmission

In order to transmit information through the wall of the storage cask ultrasonic transducers will be used due to their ability to convert electrical to mechanical energy and mechanical to electrical energy. This section will discuss the theory of ultrasonic transducer wave production and the types and materials of transducers. Methods and results of the performed tests and some radiation and temperature considerations are included. Also a summary of recommendations has been provided.

7.1 Ultrasonic Transducer Theory

Ultrasonic transducers transmit and receive high-frequency sound or acoustic waves, having a typical frequency greater than 20 kHz. The wave is able to propagate through the material in a variety of modes differentiated by the motion or direction of the particle oscillation. *Longitudinal* or *compression* waves occur when the atomic compression and expansion are in the direction of the wave travel (Figure 7.1). *Shear waves* are formed as the atoms vibrate in a perpendicular direction from the traveling direction of the signal. Shear waves do not travel as quickly through a material as do longitudinal waves.[10]

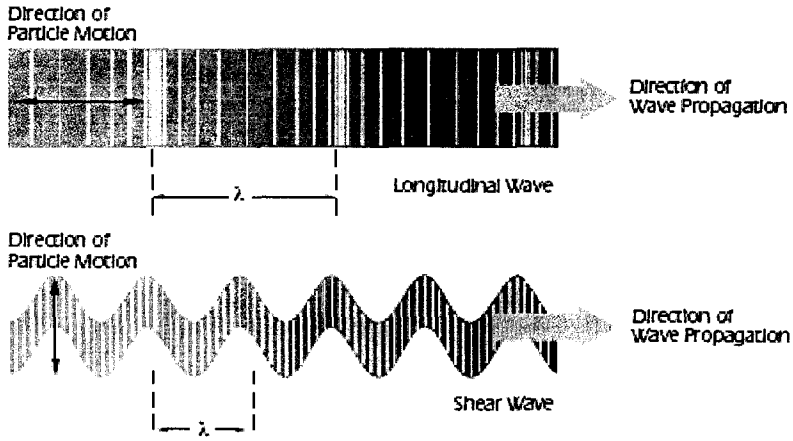

Figure 7.1 Illustration of Longitudinal and Shear Waves[11]

In the case of *Raleigh* or *surface* waves, the atoms experience vibration in an elliptical orbit on the surface of the material, reaching a depth in the material of one wavelength[10].

As the wave propagates the signal is decreased due to inelastic interactions and scattering by material defects. In order to minimize the amount of signal loss due to reflection, the impedance of the transducer should match the impedance of the material. Calculation of impedance is as follows[11]:

$$Z = \rho V \tag{7.1}$$

In the equation ρ is the material density, and V is the acoustic velocity of the wave through the material. Once the impedance is determined the fraction of the original signal which is reflected can be calculated using[11]:

$$R = \left[\frac{(Z_2 - Z_1)}{(Z_2 + Z_1)}\right]^2 \tag{7.2}$$

In the equation Z_1 denotes the impedance of one material while Z_2 is the impedance of the other material. This fraction of reflection subtracted from the original signal strength shows how much of the signal will be transmitted into the material.

In reality, transducers do not produce a single acoustic wave but rather produce many signals generated across the transducer surface. The signal detected after propagating through the material is determined by the addition of the phases of the waves produced. When the waves are completely in phase, the waveforms combine forming amplitude which is greater than either individual signal. If the waves are completely out of phase with each other, the signal is cancelled, and when they are in different but not opposite phases, an altered waveform is produced from their combination (Figure 7.2).

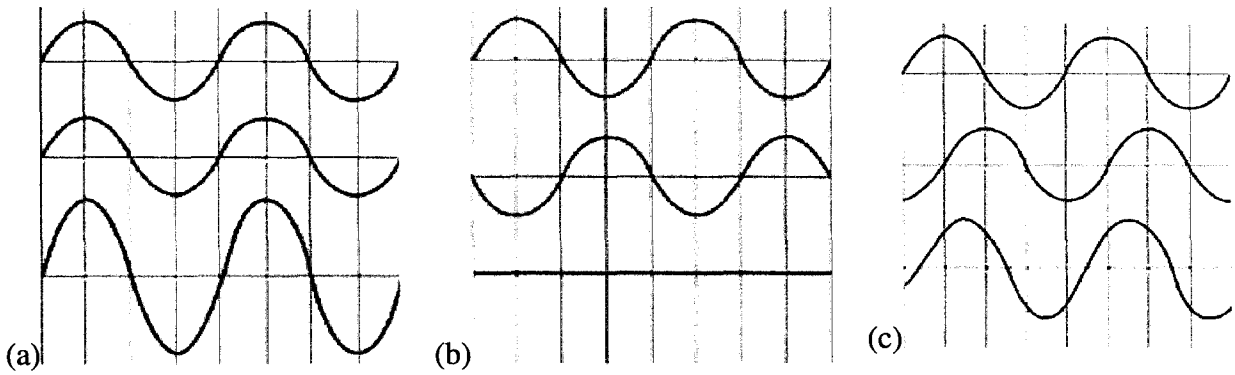

Figure 7.2 (a) In phase (b) Out of phase (c) In-between, not in or out of phase completely[10]

Due to the production of waves from several locations on the transducer surface, there is a region which contains a high concentration of wave interaction, called the *near field* (Figure 7.3). In the near field, the waves overlap and interact, producing intense fluctuations and no single, clear signal. When distance from the transducer is increased, the signal becomes more clear and uniform in the *far field.*

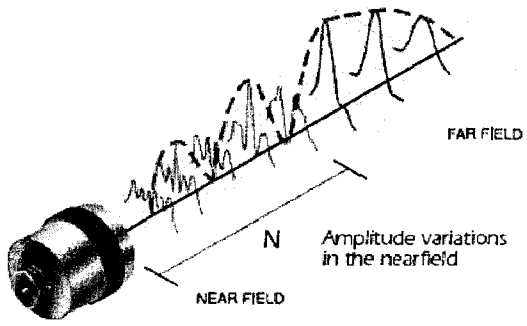

Figure 7.3 Fields produced by transducer[11]

The transition point between the near and far fields is the *natural focus* (*N*) of the transducer and is the point where the signal is at a maximum strength. The near field distance can be calculated using[11]:

$$N = \frac{D^2 f}{4c} \tag{7.3}$$

In the equation, D is the transducer (element) diameter, f is the frequency of the produced signal, and c is the velocity of the signal through the material being used as a medium. (*Appendix C*) It is recommended that a frequency be selected which produces a near field length at the approximate wall thickness.

A development that seeks to pulse the wave signals by individual or in groups ranging from 16 to 256 elements, is called *phased array pulsing*[12]. With the use of software to program timing sequences, waves can be produced in a manner in which they will combine to form a clear, strong signal. Because the signal is concentrated, it is recommended that a phased array transducer be utilized. Based on the test being performed and the type of materials used, the size of the pulsating group, or *aperture*, can be selected (Figure 7.4).

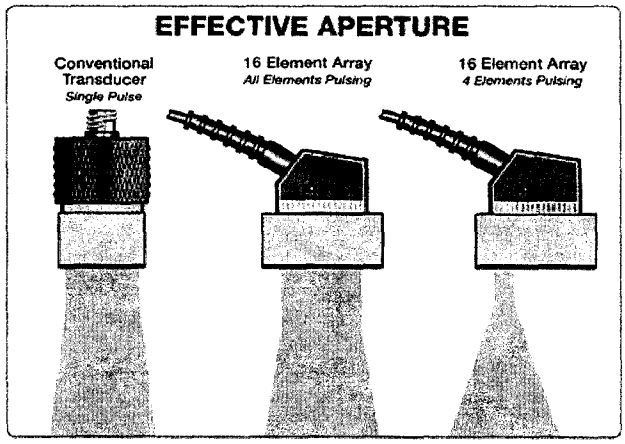

Figure 7.4 Conventional transducer pulse versus various phased array pulses[12]

As distance is increased from the transducer the projected signal diffuses in a process called *beam spread* or *divergence*[10]. Spread of the beam occurs because the material particles do not always interact in a manner that passes energy in a straight-forward path. Beam spread is the measured angle from one side of the beam to the other, and beam divergence is the measured angle from the center of the beam to the outer edge (Figure 7.5).

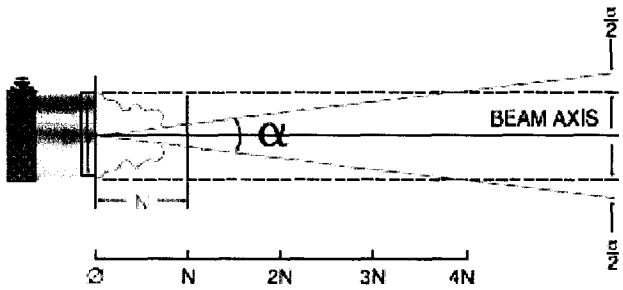

Figure 7.5: Beam spread angle[11]

Therefore the beam spread is equal to twice the beam divergence. The beam spread angle can be calculated using[11]:

$$\sin\left(\frac{\alpha}{2}\right) = \frac{.514c}{fD} \tag{7.4}$$

Where D, f, and c are element diameter, signal frequency, and signal velocity respectively. Due to the beam spread, the strongest signal will be located along the transducer center axis. By increasing the signal frequency or the aperture, or transducer diameter, the beam spread is decreased[12] (Figure 7.6).

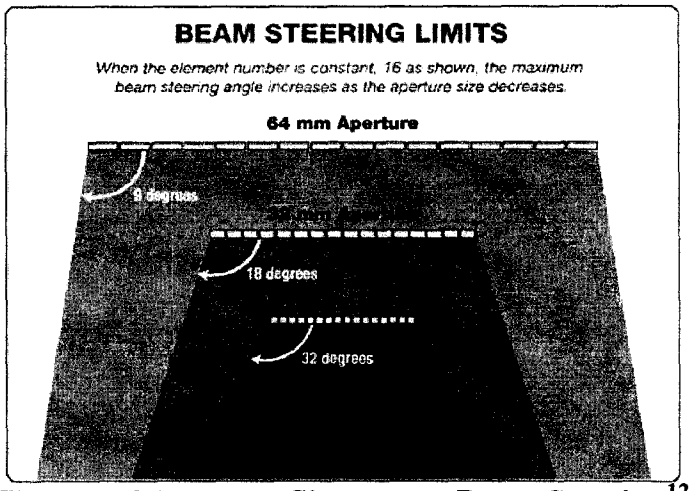

Figure 7.6 Aperture Size versus Beam Steering[12]

Although less beam spread means a higher concentration of wave intensity is transmitted, more beam spread decreases the amounts of reflection signals. Therefore, it is recommended that a frequency and small transducer diameter be selected which increases the beam spread and steering capabilities. Other factors that can contribute to avoiding impurity refraction or scattering due to grain boundaries and maintaining the signal strength are signals with longer pulses and lower frequencies[10].

In the non-destructive testing (NDT) methods, transducers are used to transmit a signal into the material an angle using an angled block instead of having the transducer surface directly contact the material at no offset angle. However, because the goal in NDT is to analyze a material for damage, impurities, or other conditions, transducer properties are selected that will best interact with these defects. When using the material as a medium in which to transmit a signal through the goal is to not interact with the flaws in the material but rather to keep the signal intensity as high as possible. Therefore, to minimize refractive processes the signal should be transmitted straight into the material, forming no offset angle between the signal transmittance direction and the intended direction of wave propagation. Another benefit of not using an entry

angle is the decrease of attenuation in the form of shear waves after the signal passes through the material and reaches the material boundary.

7.2 Types of Transducers and Components

7.2.1 Comparison of Transducers

Transducers come in a wide variety specified by intended use. Transducers are different sizes and shapes and have various designs, materials, and purposes. Electromagnetic-acoustic transducers (EMATs) are designed for high temperatures in remote locations and do not require couplant due to the use of electrical conduction and eddy currents (Figures 7.7 and 7.8).

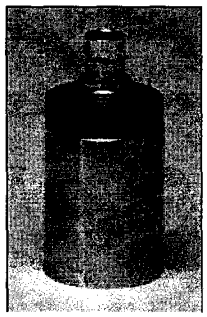

Figure 7.7 Electromagnetic Acoustic Transducer[14]

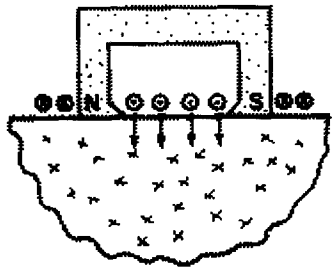

Figure 7.8 Cross-sectional view of a tangential field EMAT for exciting polarized longitudinal waves propagating normal to the surface[10]

Because the EMAT does not require a couplant to transmit a signal, the measurements are considered more consistent with less error than piezoelectric transducers. However, the signals produced by EMATs are weaker than those produced by piezoelectric transducers. Also strong magnetic fields and large currents are necessary to use an EMAT[10].

Contact transducers are used in direct contact with the surface of a material and typically produce a longitudinal wave (Figure 7.9). They are provided with a wear face that matches most metals in acoustic impedance. Most contact transducers are for continuous use but only on materials up to a temperature of 50°C[14].

Figure 7.9 Contact Transducer Dimensions (a) diameter (b) thickness[14]

Another type of transducer which can be used on surfaces with a maximum temperature of 426.7°C at 5MHz and below, are the corrosion gage duals, or dual element transducers (Figure 7.10). Like most transducers the dual element transducers are encased in 303 stainless steel, however they contain both a transmitting and a receiving element[14].

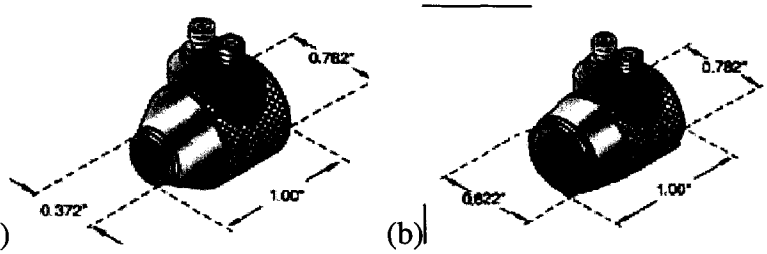

(a) (b)

Figure 7.10 Dual Element Transducers (a) 0.25 inch element size (b) 0.5 inch element size[14]

Although the dual element transducers can be used on rough or curved surfaces, they can only remain at temperatures from 93.3-426.7°C for about 10 seconds, at which they need over a minute to cool down[14].

The delay line transducers are also designed for use in temperatures up to 482.2°C (Figure 7.11). Delay line transducers are designed to receive a signal after a specified amount of time from initial signal production. They have a small piece of plastic or epoxy on the surface of the transducer[14].

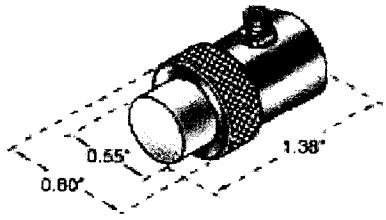

Figure 7.11: Delay Line Transducer[14]

The delay line transducer is recommended due to the temperature of use. However, a specially designed transducer would overcome the disadvantages of the delay line, which include optimization with thin materials.

7.2.2 Piezoelectric Material

A transducer converts an electric signal into a vibrational, mechanical wave using polar, piezoelectric material which has the ability to deform when exposed to an electric signal and conversely produces an electric signal when deformed, called the *piezoelectric effect*. The amount of deformation is proportional to the field strength[13]. In order to pass current, the piezoelectric material is connected to electrodes on opposite faces (Figure 7.12).

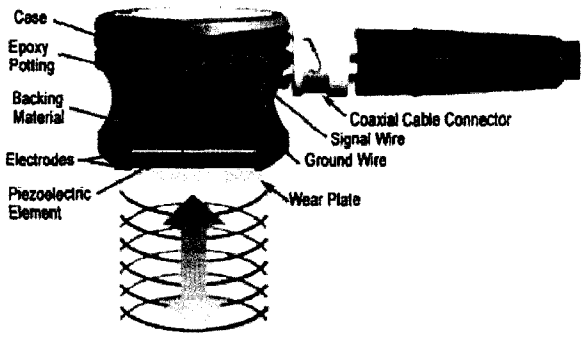

Figure 7.12 Transducer Components[10]

If a current is quickly applied and then removed, the piezoelectric material deforms and expands in a response fast enough to produce an ultrasonic wave[13]. The thickness of the piezoelectric crystal determines the wavelength of the signal as well as the voltage and the amount of time the voltage can be applied. The wavelength of the ultrasonic wave produced is equal to twice the crystal thickness[10]. For each millimeter of piezoelectric transducer thickness, a limit of *excitation* voltage of 50 volts should be used. Because lower frequency transducers are thicker, a higher voltage can be applied than to high frequency transducers. The voltage supplied to the transducer is lower if a continuous signal is used[11]. The central frequency that is specified for each transducer gives information about the characteristics of the transducer. For example, transducers with frequencies in the low MHz range produce a signal with more energy and more material penetration than those of 15 MHz and up[10]. Typically piezoelectric crystals are ceramics due to their ability to use low voltage and perform at high temperatures such as 300°C[10].

A backing material is included in the transducer as a damper for the piezoelectric crystal after a pulse has been generated. The properties of the backing material affect the bandwidth and

the sensitivity of the instrument. Holding the backing material and the piezoelectric crystal is an epoxy, or polymer mixture.

7.2.3 Couplant Material

Couplant material is used to fill the air gap between the transducer and material surface so that acoustic waves can enter the material. Due to the drastic difference in impedance between the transducer surface and air, without couplant material nearly all of the signal would be completely reflected back in to the transducer[10].

The type of couplant that is used is determined based on the characteristics of the system. It is recommended that couplants be selected which will minimize impedance between components and can withstand the cask environment. For example, most couplants are characterized by temperature for use.

Table 7.1 Couplant Types and Characteristics[15]

Couplant Material	Temperature
Propylene Glycol	150 C
Glycerin	90 C

Although not listed in the table, Olympus Panametrics-NDT also has a couplant for a temperature maximum of 315.6°C[15].

7. 3 Testing Methods and Results

Using properties of type 1020 carbon steel and type 347 austenitic stainless steel (*Appendix A*) values were calculated for the time of flight, or time for the signal to travel through the plate, material impedance, and the beam spread angle at 2.3 MHz (Table 7.2). Time of flight is equal to twice the material thickness divided by the velocity. Impedance was calculated using Equation 7.1, and Beam Spread Angle was found using Equation 7.4.

Table 7.2 Calculated values for 1020 carbon steel and 347 austenitic stainless steel

Material	Material Thickness	Density	Longitudinal Velocity	Time of flight	Impedance (Z)	Beam Spread Angle °
	(m)	(kg/cu. m.)	(m/s)	(s)		(freq = 2.3 MHz)
Steel, 1020	0.015875	7861.1	5890	5.39E-06	4.63E+07	11.89
austenitic stainless Steel, 347	0.015875	8027.2	5740	5.53E-06	4.61E+07	11.59

In order to realize the frequency which produces a near field length closest to the plate thickness, calculations were made for both steels over a range of 0.5-15 MHz (*Appendix B*). The relationship between frequency and near field length is linear (Figure 7.13). This property supports the theory that with increasing frequency the beam spread decreases, therefore the near field length increases.

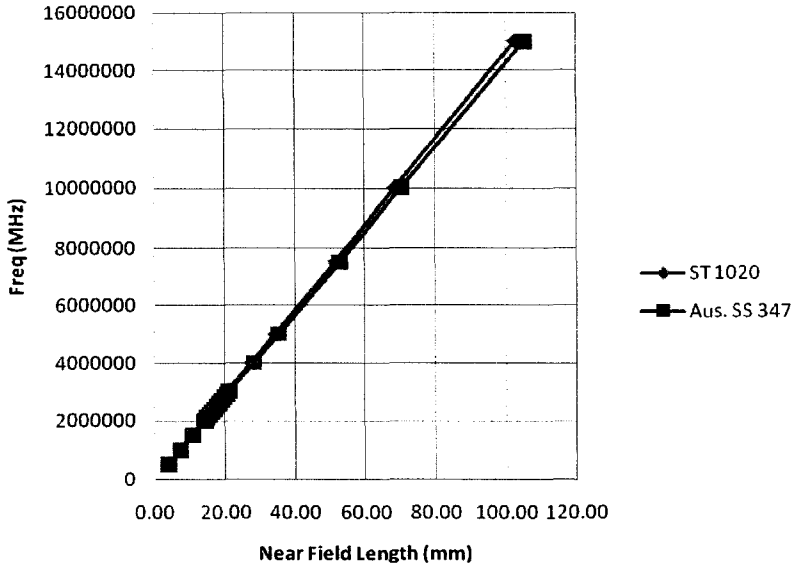

Figure 7.13 Frequency vs Near Field Length

Because the cask wall is 15.875 mm (5/8 inch) thick, more values were calculated for the frequency range that produced near field lengths close to the wall thickness. Even a change in frequency of 0.1 MHz changes the near field length by approximately 0.03 inches (Figure 7.13).

Experiments were performed on the transducers to test the amount of signal being received through steel plates with various couplants. Tests were also performed to compare signal loss to plate thickness and to transducer-to-transducer offset. These tests were performed in order to provide an estimate for the amount of power needed to provide a defined signal, to approximate the precision needed in alignment of the transducers on each side of the cask wall, and to compare types of couplant for producing the maximum signal.

Experiments included the use of a function generator, oscilloscope, various couplant materials, stainless steel plates (3/8 inch (9.525 mm) and 3/4 inch (19.05 mm) thick), a C-clamp, an Olympus Panametrics-NDT contact transducer: C109-RM, 5MHz, 0.5 inch element diameter (0.7 inch (17.78 mm) face diameter 0.63 inch (16.00 mm) thickness), 303 stainless steel case (*Appendix A*). One transducer was connected to the function generator, and the other was

connected to the oscilloscope. In all tests a sine wave with 3-volt amplitude, 6-volt peak-to-peak, was produced by the function generator. During testing a clamp was used to keep the transducers in contact with the steel plate in order to maintain a consistent pressure (Figure 7.14). As pressure was increased the signal transmitted through the plate also increased.

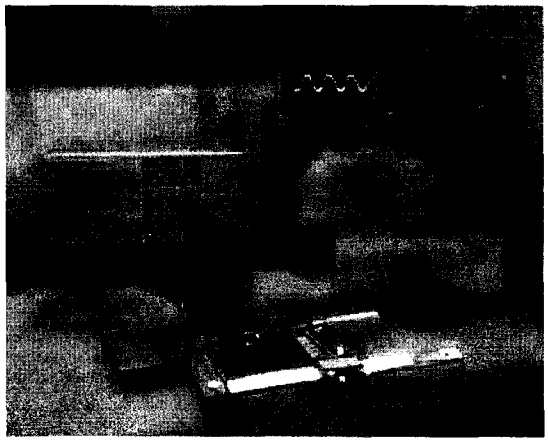

Figure 7.14: Experimental Setup with 3/8 inch SS plate

The first experiment was performed using Dow Corning 200 fluid, 30,000 cs (liquid silicone)[23] with one 3/8 inch (9.525 mm) smooth stainless steel plate. A 3-volt peak-to-peak sine wave was applied to the transducer and transmitted through the steel plate to the other transducer. The resulting voltage from the receiving transducer was measured using an oscilloscope. The voltage response was measured as the frequency was cycled by 0.1 MHz from 2 to 7 MHz (Figure 7.15). In order to visualize the voltage gain at each frequency the response in decibels was calculated[11]. The plotted data are provided (*Appendix D).*

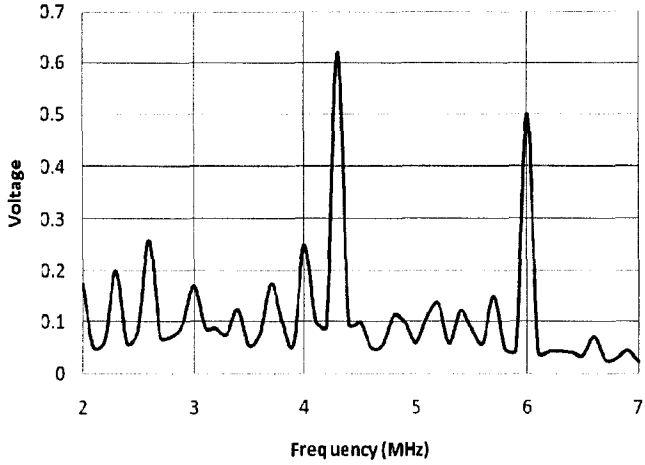

Figure 7.15 Voltage vs Frequency for 9.525 mm plate & Liquid Silicone Couplant

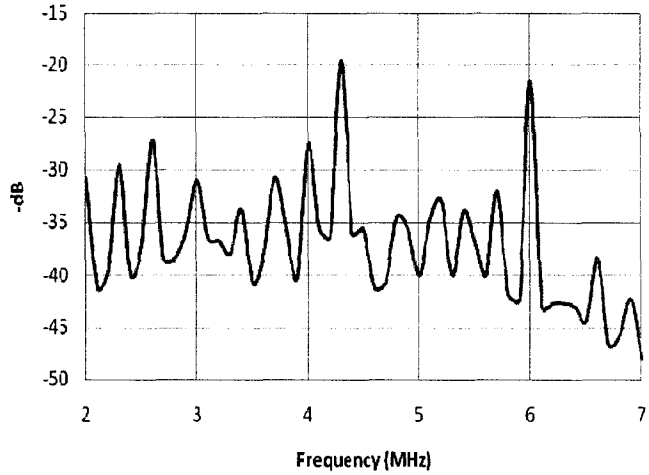

Figure 7.16 Voltage gain (-dB) vs Frequency for 9.525 mm plate & Liquid Silicone Couplant

The decrease from a 6-Volt peak-to-peak signal to a maximum value of approximately 0.62 volts, about 10.3% of the original signal, occurs at 4.3 MHz and shows that significant attenuation is occurring. Because the flash point of liquid silicone oil (30,000 cs) is approximately 326.7°C[23] or a little higher, it may or may not be useful as a couplant in the cask environment, depending on drying temperatures and duration.

The next experiment also involved voltage and voltage gain response to frequencies ranging from 2.0 to 7 MHz transmitted through a 3/8 inch (9.525 mm) stainless steel plate (Figures 7.17 and 7.18). The plotted data are provided (*Appendix E*). However, for the second procedure petroleum jelly was used as a couplant between the transducer and steel surfaces. The maximum percentage of the signal recovered was approximately 9.6% of the original signal also at 4.3 MHz. Although the voltage response is comparable to the liquid silicone, the flash point of petroleum jelly, approximately 185°C[16], makes it unusable in high temperature situations; however experimental use provides a comparison between the types of couplants.

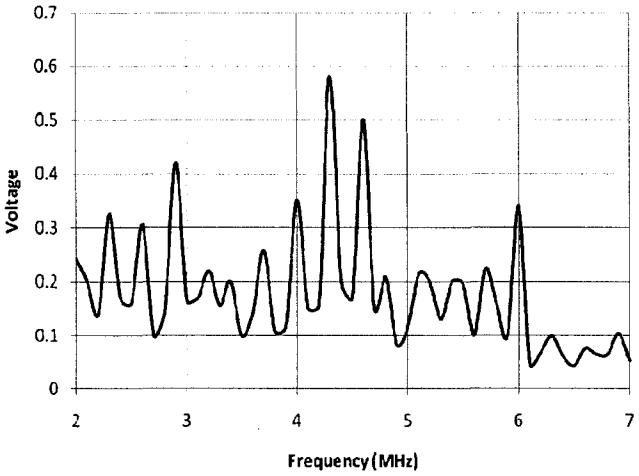

Figure 7.17 Voltage vs Frequency for 9.525 mm plate & Petroleum Jelly Couplant

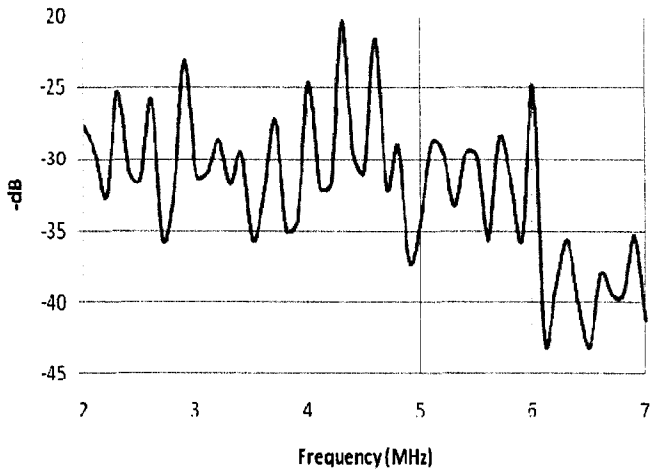

Figure 7.18 Voltage gain (-dB) vs Frequency for 9.525 mm plate & Petroleum Jelly Couplant

Another couplant, magnesium hydroxide ($Mg(OH)_2$), was also used to measure voltage and voltage gain response to frequencies ranging from 3 to 5.3 MHz (Figures 7.19 and 7.20). The plotted data are provided (*Appendix F*). The melting point of $Mg(OH)_2$, which is approximately 2800°C[17], is well in the range of spent fuel storage casks, but the largest signal received was only approximately 6.2% of the original voltage also at 4.3 MHz.

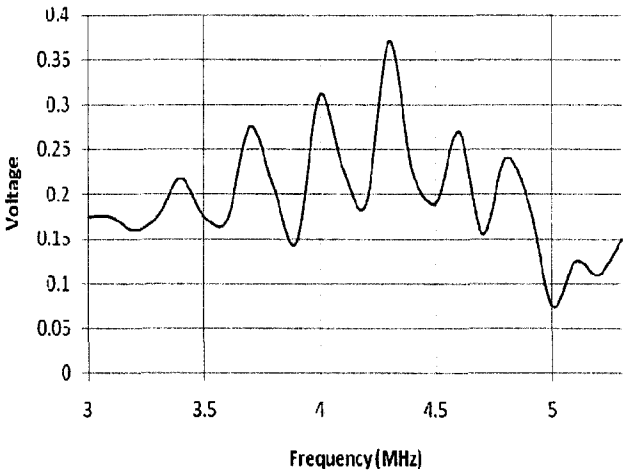

Figure 7.19 Voltage vs Frequency for 9.525 mm plate & $Mg(OH)_2$ Couplant

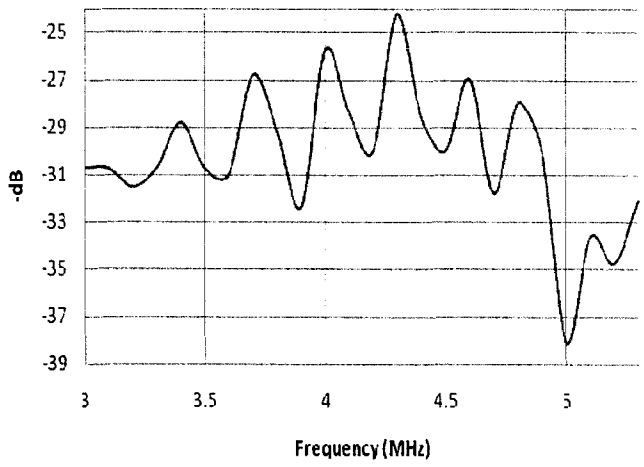

Figure 7.20 Voltage gain (-dB) vs Frequency for 9.525 mm plate & $Mg(OH)_2$ Couplant

Comparison of the couplants used in voltage and voltage gain response to frequency illustrates that liquid silicone oil has a higher maximum reponse (Figure 21). Although the response using the petroluem jelly is higher for most frequencies than for liquid silicone oil, the petroleum jelly has a lower flash point and is not recommended for the cask environment.

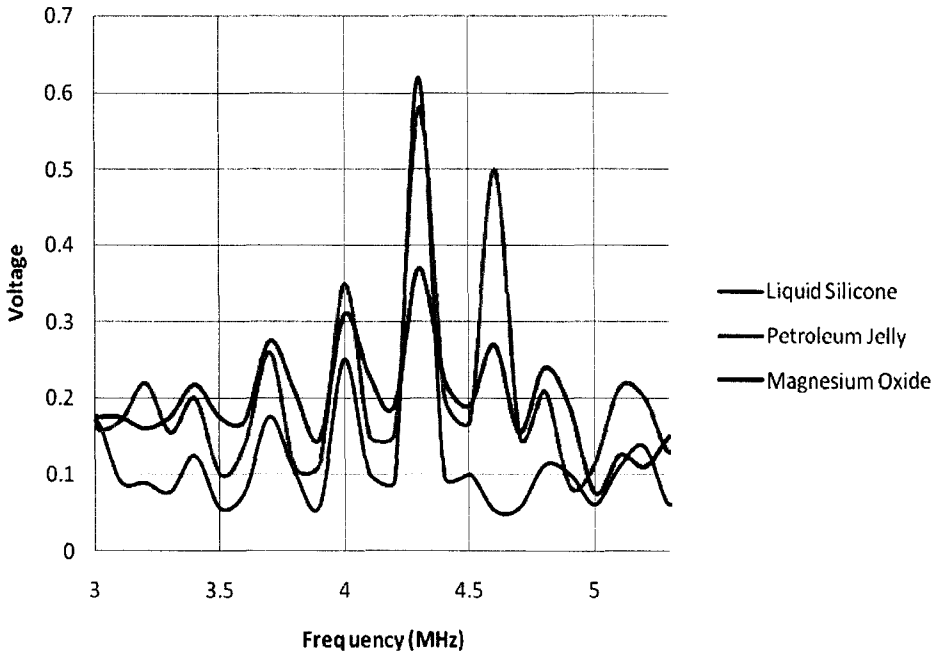

Figure 21: Comparison of voltage response versus frequency for couplants on 9.525 mm plate

For the next experiment, the voltage and voltage gain responses to frequencies ranging from 1.7 to 6 MHz was measured for a 6-volt peak-to-peak signal through a smooth area of a 6/8 inch (19.05 mm) stainless steel plate. (Figure 7.22 and 7.23). The plotted data are provided (*Appendix G*). Because of the material properties and due to the largest signal recovery in previouis procedures, liquid silicone oil was used for all of the following procedures.

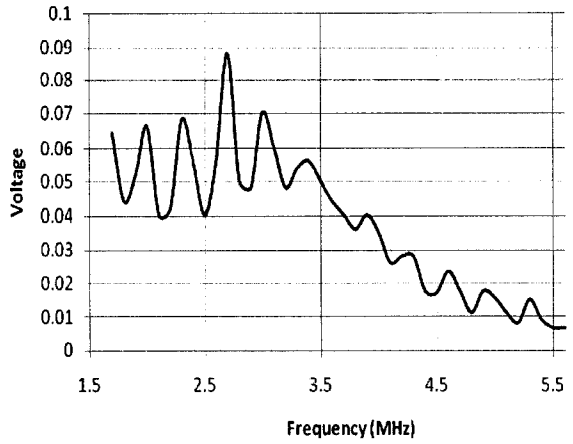

Figure 7.22 Voltage response vs Frequency for 19.05 mm plate & Liquid Silicone Couplant

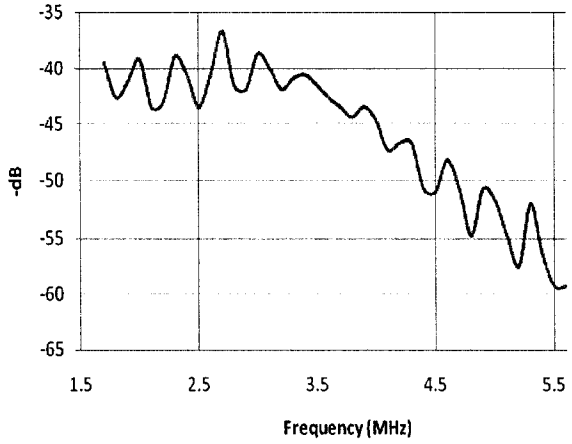

Figure 7.23: Voltage gain (-dB) vs Frequency for 19.05 mm plate & Liquid Silicone Couplant

Although 10.3% of the original signal was recovered through the 3/8 inch (9.525 mm) plate, a maximum recovery of 2.8% occurs at 4.3 MHz through a 6/8 inch (19.05 mm) steel plate. Because the percentage did not half with double plate thickness, the results show that the signal strength decreases through the plate in an exponential fashion rather than linearly.

To show not only the relationship between plate thickness and voltage response but also the comparison between rough and smooth plate addition, the next procedure was performed. A 3-volt peal-to-peak sine wave was transmitted through the steel at a constant 4.3 MHz. First an unpolished, rough surface 3/8 inch (9.525 mm) plate was connected to the transducers with the liquid silicone couplant, and the voltage response was measured. Then two plates were connected to each other and to the transducers using liquid silicone, forming a total thickness of 6/8 inch (19.05 mm), and the voltage response was measured again (Figure 7.24). The plotted data are provided (*Appendix H*).

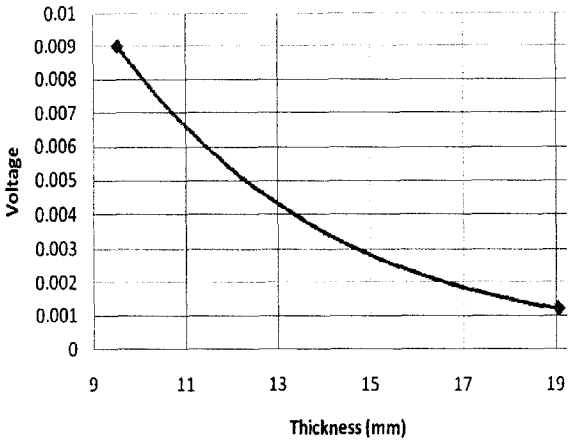

Figure 7.24 Voltage response vs Plate thickness (rough plate with rough plate addition)

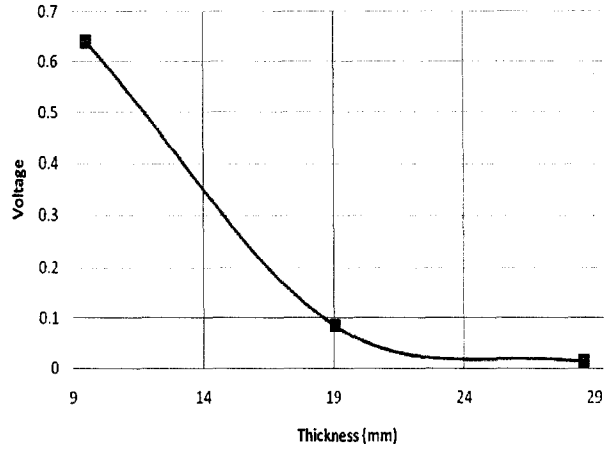

Figure 7.25 Voltage response vs Plate thickness (smooth plate with rough plate addition)

Due to the loss of signal from the addition of one rough plate, it was concluded that an undetectable signal would be produced if another rough, 3/8 inch plate was added.

Next the voltage response was measured at 4.3 MHz through a polished, smooth, 3/8 inch plate. Then the voltage response was measured as each rough surface, 3/8 inch plate was added, for a total of 3 plates or a thickness of 1.125 inches (Figure 7.25). The plotted data are provided (*Appendix I*). Comparison between the signal detected through the rough 3/8 inch plate (Figure 7.24), 0.009 volts, and the smooth 3/8 inch plate (Figure 7.25), 0.64 volts, demonstrates the importance of the surface texture. As expected from the previous percentage decrease from 10.3% maximum value to a 2.8% maximum value, the attenuation appears to be exponential with plate thickness.

The next procedure was performed to relate transducer-to-transducer offset distance to the voltage and voltage gain responses for a 6-volt peak-to-peak, sine wave at 4.3 MHz (Figures 7.26 and 7.27). The plotted data are provided (*Appendix J*). The setup involved the use of one,

smooth, 3/8 inch (9.525 mm) plate and liquid silicone couplant. For the first measurement with zero offset, the transducers were placed at the edge of the plate. To increase the offset distance, one of the transducers was left in place at the edge of the plate while the other transducer was moved to the next measured distance.

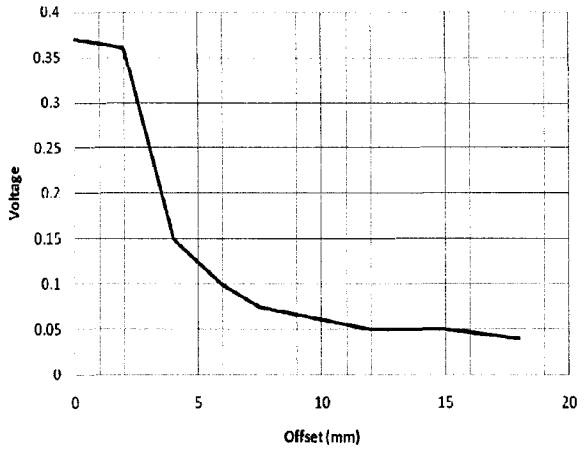

Figure 7.26 Voltage Response vs Transducer-to-Transducer Offset distance

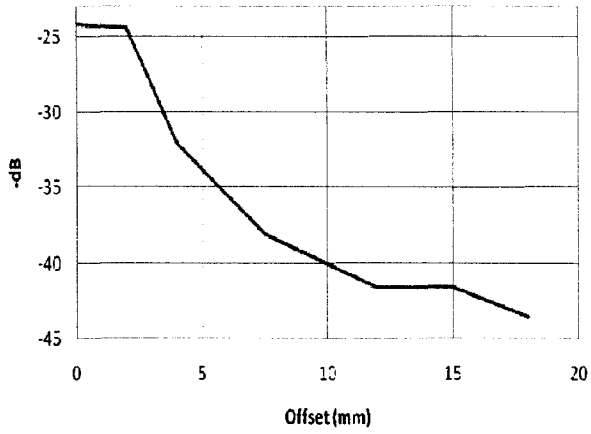

Figure 7.27 Voltage gain (-dB) vs Transducer-to-Transducer Offset distance

The results illustrate the importance of transducer alignment in that the greatest signal recovery occurred where the transducers were directly opposite.

7.4 Radiation and Temperature Considerations

Due to the range of material selections available for use in transducers, some estimates are required in order to consider the exposure to high temperatures and radiation a transducer would experience inside a spent fuel cask. The most durable component of the transducer, the case which is typically stainless steel, has an extremely high melting point. Also because stainless steel is used as shielding for the cask, it provides some shielding to the inner

components of the transducer. Therefore the components which are of most concern due to lower melting temperatures and inability to maintain composure at high radiation levels are the backing materials, epoxy mixtures, and the piezoelectric or piezocomposite materials. Although the properties of the internal transducer components vary from type to type, the components are generally of the same nature.

Amplitude response versus frequency results for a lithium niobate piezocomposite transducer over a range from 25 to 400°F shows that although amplitude does change with temperature, the signal is fairly consistent[18]. Although the internal transducer materials may suffer some damage, the transducer is still effective.

In a radiation damage study on quartz fibers, one of the common piezoelectric crystals, the damage was not severe until several Mrad were absorbed[19]. Because the dose that will be absorbed during the lifetime of the equipment inside the cask is estimated around 1 Mrad (10 kGy), the previous study[19] suggests that the piezoelectric crystal will suffer very little damage due to radiation.

Some studies show that although the piezoelectric materials may withstand high radiation, the thermal effects caused by the radiation may prove to be the most serious consideration. Some tests have been performed on the melting temperatures of polymers versus absorbed dose[20] (Figure 7.28).

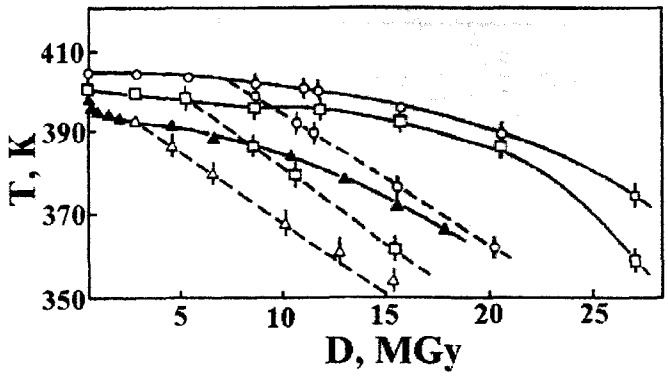

Figure 7.28 Melting temperatures from polymer samples versus absorbed radiation Ionizing Radiation and Polymers Ed. Betz, N., Le Moel, A. September 2000 Briskman, B.A. *Radiation effects in thermal properties of polymers. An analytical review. I. Polyethylene*[20]

Although the initial melting points of the specific polymers tested were lower than needed for high temperature environments, the general trend is still observed: with absorbance of radiation, the melting points of polymers decrease. Tests of other polymers confirm the trend[12] (Figure 7.29). The polymers which initially had high melting temperatures experienced a decrease as radiation was absorbed.

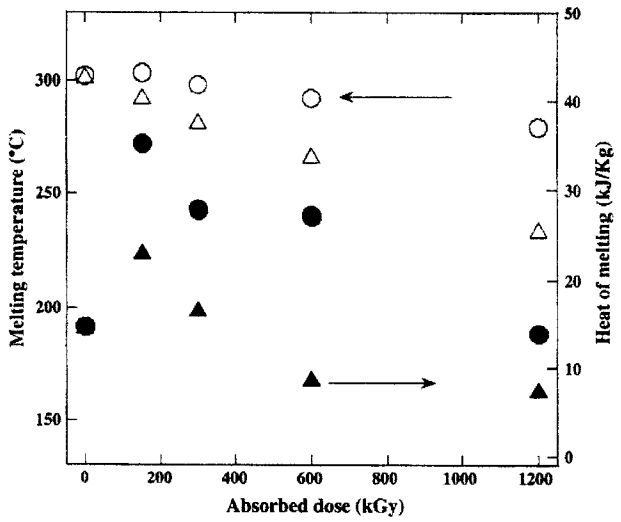

Figure 7.29 Melting temperature and heat of melting for polymers versus absorbed dose Ionizing Radiation and Polymers Ed. Güven, O. September 2006 Kakigi, T., Oshima, A., Miyoshi, N., Katsuyoshi, M., Fujii, K., Mitani, N, Urakawa, T., Sato, Y., Matsuura, A., Li, J., Miura, T., Katoh, E., Washio, M. *Study on chemical structures of poly (tetrafluoreoethylene-co-perfluoroalkylvinylether) by soft-EB irradiation in solid and molten state*[21]

Dose not only affects melting temperatures of polymers but also the degree of cross linking that is experienced[22] (Figure 7.30). As radiation is absorbed by the polymer, more cross linking is encountered. Cross linking relates to the elasticity and tensile strength of a polymer; the higher the degree of cross linking, the less flexible the material becomes. This is of great importance in application to the backing material, which is used as a damper for the piezoelectric or piezocomposite. When the backing material becomes more constrained, the vibration will be dampened more quickly.

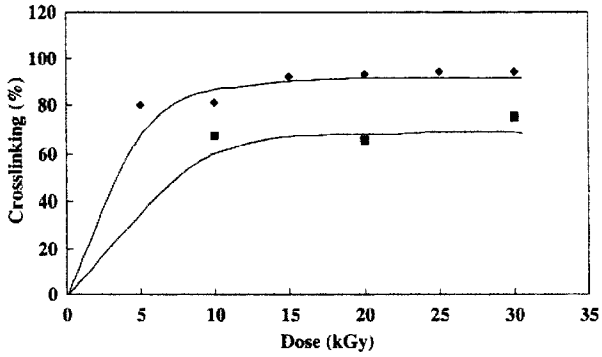

Figure 7.30 Crosslinking percentage in polymer as a function of absorbed dose by gamma irradiation (◆) Ionizing Radiation and Polymers Ed. Güven, O. September 2006 Burillo, G., Briones, M., Adem, E. *IPN's of acrylic acid and N-isopropylacrylamide by gamma and electron beam irradiation*[22]

7.5 Summary of Recommendations

The following considerations and recommendations are made after analysis of the transducer and its material components.

According to theory and calculations, a frequency should be chosen that produces a near field length that is approximately the thickness of the material being transmitted through in order to maximize the output signal. Also the frequency should be as low as possible so that more penetration of the material is possible and less interaction with material defects occur.

To benefit from the use of additive wave phased in providing a stronger signal, a phased-array transducer could be used. In order to allow for less signal loss to reflection and a more concentrated signal along the center-line of the transducer through beam spreading, the diameter should be minimized. The transducer should be selected which can tolerate the temperature range of the environment and can be shielded to withstand the radiation. For temperatures such as the spent fuel cask present, the use of a delay line transducer or another transducer with high temperature potting materials may be possible.

In order to minimize material defect interaction and the distance of signal path, therefore decreasing signal loss, the signal should be transmitted directly into the material at no offset angle between transmission direction and wave path.

A couplant must be chosen which minimizes the impedance differences. Also the couplant should have favorable properties over the temperature range of the environment. The Dow Corning 200 fluid 30,000 cs is a high viscosity liquid which may be used considering the flash point occurs at greater than 326.7C[21].

Because the signal strength and the waveform are attenuated as the wave travels, the cable length between the transducer and the previous device should be minimized. Also to aid in signal transmission, the impedance of the cable should match the circuit and the transducer. Because shielding will influence the impedance of the cable and the radiation of the signal, the cable should be provided with a shielding material that best suits the cask environment. Also the capacitance of the cable should be considered; for ability to perform at high speeds, the capacitance must be low. Lastly, both the cable and its shielding need to be able to withstand the temperature of the environment.

8 Radiation Shielding

Because of the continued decay of the nuclear fuel stored in the spent fuel cask, the environment inside the vessel is subjected to high levels of radiation, mainly in the form of neutron and gamma radiation. The primary long-lived neutron sources are from the spontaneous fission of Cm-242, Cm-244, and Cm-246 and (α,n) reactions from Pu-238, Cm-242, and Cm-244. The gamma radiation is emitted by 70 primary fission products as well as activated fuel assembly components.[2] The ORIGEN-ARP SCALE5.1 module was used to determine the

relative decay heat and neutron and gamma fluxes in a standard NUHOMS 24PL cask. The design basis PWR spent fuel for the NUHOMS 24PL cask is a 24 fuel assembly array with average burnup of 45,000 MWd/MTU. The initial fuel enrichment is 4.0 weight percent U-235 and each assembly contains 0.475 MTU. The minimum cooling time before storage is 5 years.[2] The fuel assemblies were modeled as Westinghouse 15x15 fuel pin assemblies. Plots of total decay heat and gamma decay heat over 50 years of cooling time are shown in Figures 8.1 and 8.2. Figure 8.1 shows that decay heat decreases nearly exponentially in the first 5 years (before it is placed in the cask). It then cools less quickly from 5 to 10 years and then remains relatively constant for the remaining storage period. Figure 8.2 shows that gamma decay heat experiences the same trends as total decay heat since almost all decay heat comes from gamma radiation.

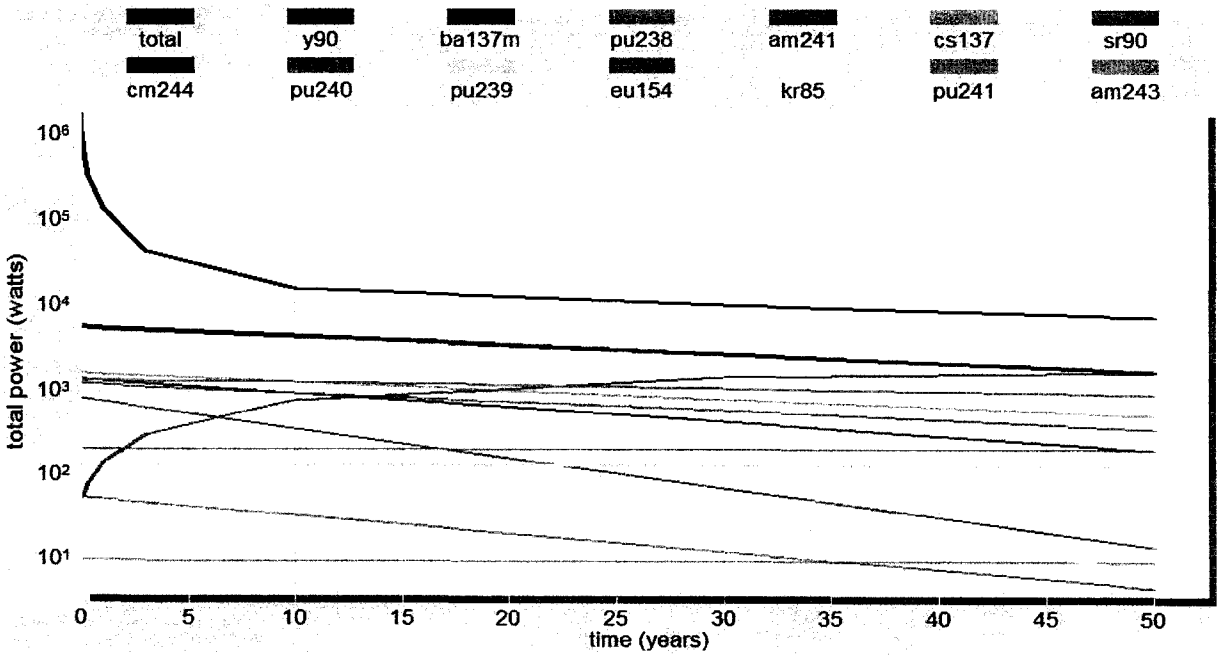

Figure 8.1 Total decay heat versus cooling time for NUHOMS 24PL cask

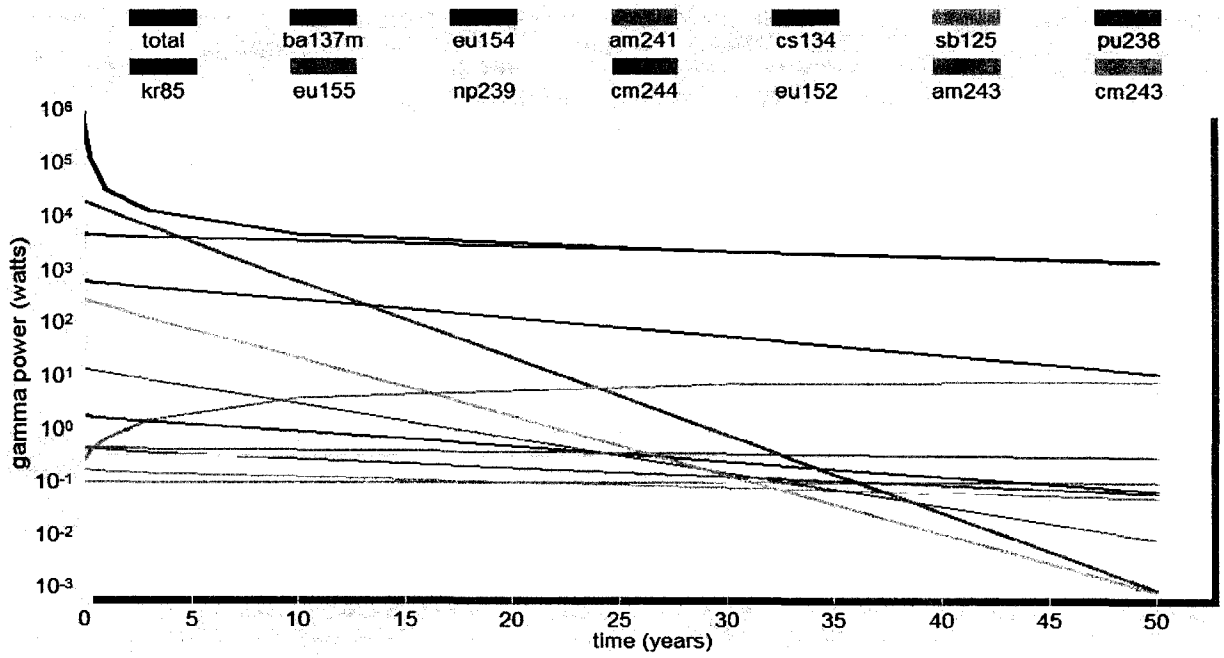

Figure 8.2 Gamma decay heat versus cooling time for NUHOMS 24PL cask

The total activity of the actinides and fission fragments were also plotted to determine the relative levels of radiation versus cooling time. Figure 8.3 shows that activity follows the same trends as decay heat and that after 10 years of cooling time (5 years in the cask) the total activity decreases at a steady rate of approximately 6.2×10^{15} Bq/year.

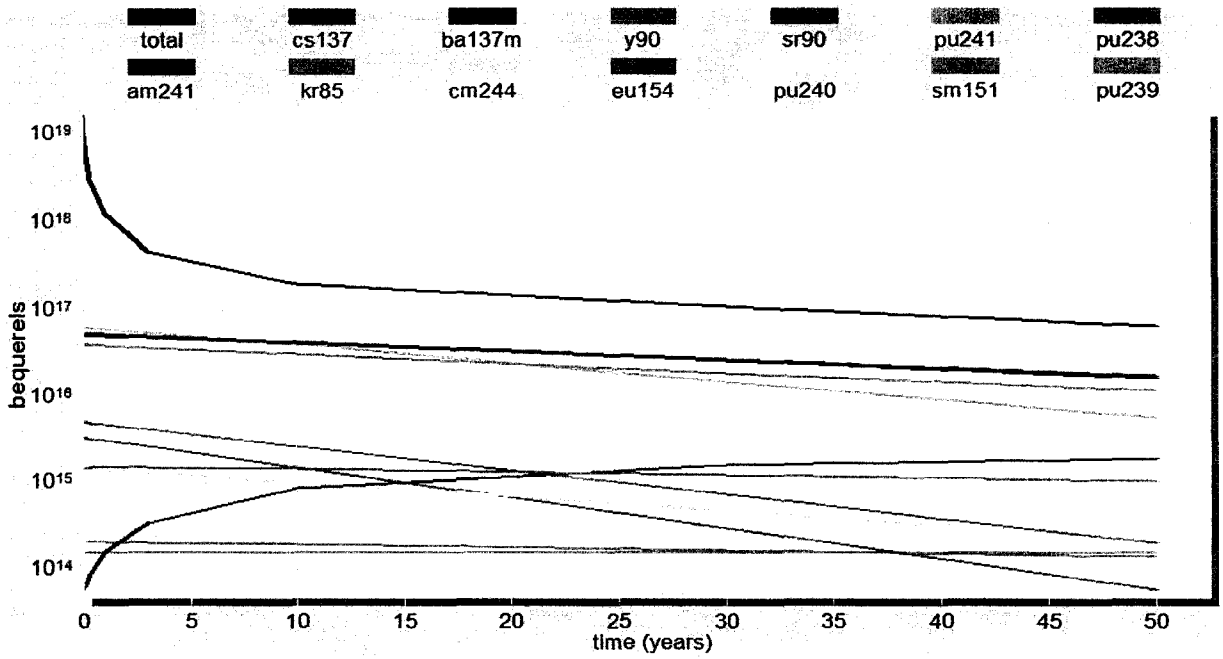

Figure 8.3 Actinide and fission fragment activity versus cooling time for NUHOMS 24PL cask

8.1 Radiation Effects and Protection

Neutron and gamma radiation are harmful to electronics because of their ability to degrade the performance of the individual components of a system. Gamma radiation ionizes particles in the electronic components, causing atomic displacements or shifts in the lattice structure that is crucial to electrical conduction. In general, this causes capacitors, circuit-board material, and other insulators to "leak" electronic signals. Gamma radiation can also induce current in circuitry via the photoelectric effect that causes noise or false signal generation. Neutron radiation's greatest effect on electronics is its ionization and activation of circuitry materials. The level of neutron radiation on electronics, however, is significantly lower than the effects of gamma radiation.

To protect against the incident radiation, electronics are protected by radiation hardening and shielding. Radiation hardening is the protection of electronics through changes in the manufacturing process and is usually applied to previously available commercial electronics. Hardening is accomplished by directly shielding electronic components, substituting normal semiconductor material for more insulating material, incorporating particle-absorbing materials such as boron into the design, and by introducing redundancy in components.

The second step in radiation protection is the use of direct radiation shielding. This involves placing radiation-absorbing material between the radiation source and the device to be shielded. For neutron shielding, low atomic mass number materials such as hydrogen are used to maximize neutron energy loss per collision event. Water and polyethylene are very effective neutron absorbers because of their high hydrogen concentrations. Neutron absorbing materials, such as boron, are also highly effective at shielding neutron radiation. Gamma radiation is best shielded with high atomic mass materials that also have high densities. Because of this, lead and tungsten are the most widely used materials for gamma radiation shields although tungsten can be prohibitively expensive.[24]

8.2 Shielding Calculations and Results

The shielding calculations for the cask were performed using the SCALE5.1 modular computer analysis software package. The SAS2 module was used for depletion, source term, and source spectra calculations. This module provides a pseudo 2-D analysis using the 1-D neutron transport code XSDRNPM. The ORIGEN-S module is accessed through the SAS2 module to perform the point-depletion calculations to produce the burnup-dependent fuel compositions. As previously mentioned, the design basis for the NUHOMS 24PL cask is 24 PWR fuel assemblies

with 4.0 weight percent initial U-235 enrichment, 45,000 MWd/MTU burnup, and five years cooling time. The bounding assembly design in terms of decay heat and activity is the Babcock and Wilcox 15x15.[2] It should be noted that although the Babcock and Wilcox assembly is the most reactive, the previous ORIGEN calculations used Westinghouse fuel assbmlies to obtain a general basis for how decay heat and activity change over time. Therefore, the shielding model was based on the Babcock and Wilcox fuel assembly design information listed in Table 8.1 for the SAS2 calculations.

Table 8.1 B&W 15x15 fuel assembly specifications[2]

Parameter	Value
Maximum number of fuel rods	208
Fuel density, % theoretical	96.0%
Quantity of guide tubes	16
Quantity of instrument tubes	1

Parameter	Inches	cm
Pellet diameter	0.3735	0.9487
Active fuel length	142.3	361.4
Plenum Length	8.73	22.17
Cladding thickness	0.025	0.0635
Fuel rod OD	0.43	1.0922
Fuel rod pitch	0.568	1.44272
Guide tube OD	0.53	1.3462
Guide tube thickness	0.032	0.0813
Instrument tube OD	0.493	1.2522
Instrument tube thickness	0.052	0.1321

The design basis specified a burnup of 45,000 MWd/MTU but did not specify MW/assembly or the number of days spent in the reactor. Therefore, a parametric study was performed to determine the worst case scenario based on MW/assembly and days of irradiation. The combinations ranged from 20 MW/assembly and 1068.75 irradiation days to 14 MW/assembly and 1526.79 irradiation days. The results are shown in Figures 8.4 and 8.5 and Table 8.2 below.

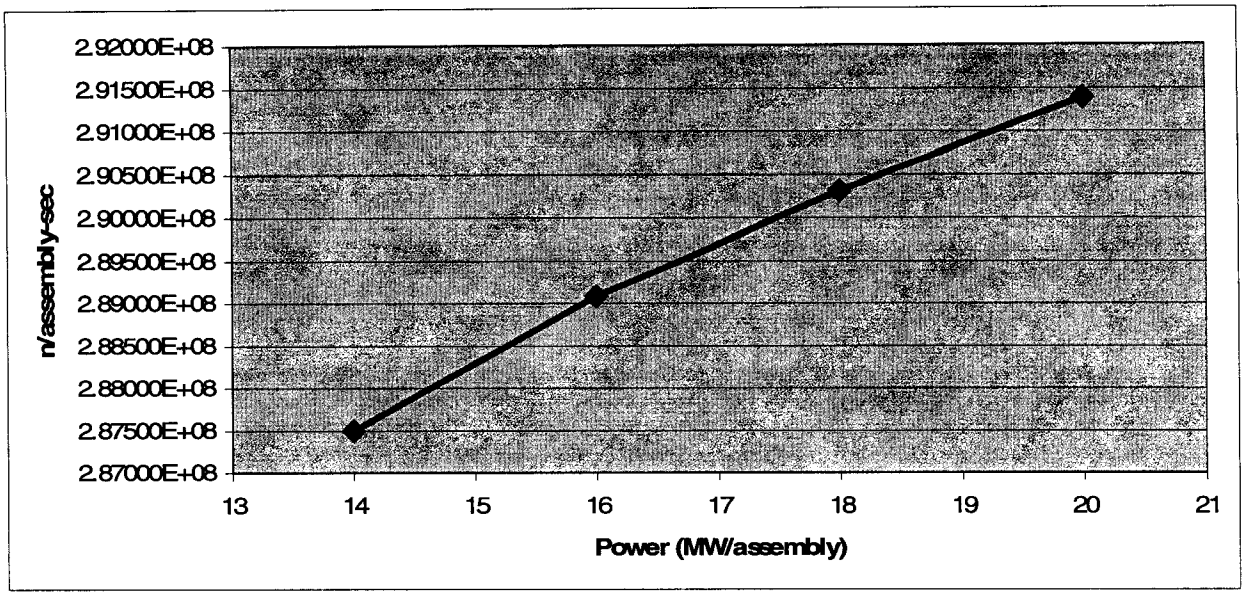

Figure 8.4 Neutron source term versus assembly power

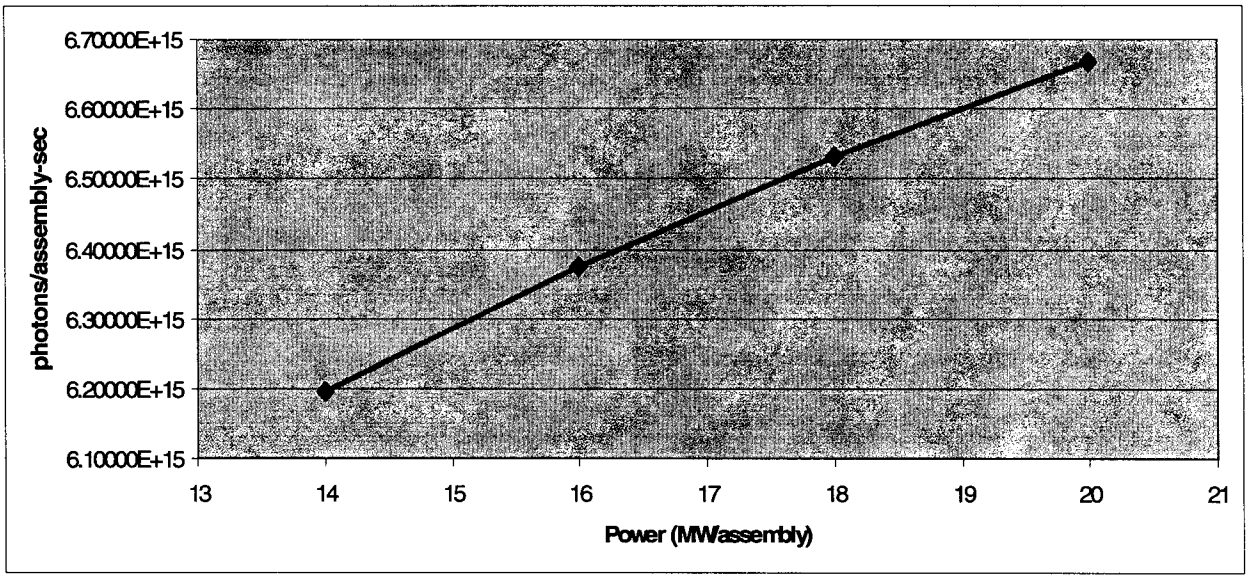

Figure 8.5 Photon source term versus assembly power

Table 8.2 Source term parametric study results

Burnup MWd/MTU	Power MW/assembly	Days in Core	Cooldown Years	neutrons/assembly-sec	gamma/assembly-sec
45000	20	1068.75	5	2.91E+08	6.67E+15
45000	18	1187.5	5	2.90E+08	6.53E+15
45000	16	1335.938	5	2.89E+08	6.38E+15
45000	14	1526.786	5	2.88E+08	6.20E+15

The results in Table 8.2 show that although the source terms vary little by changing the power per assembly, the highest terms resulted from 20 MW/assembly and 1068.75 days in the core. Therefore, this combination was used on all subsequent SAS2 calculations.

Next, source terms and source spectra were calculated for 5, 10, 20, 30, and 40 years cooling times using the SAS2 module. A sample input deck for the SAS2 calculations is shown in Appendix P. The results are shown in Figures 8.6 and 8.7 and in Table 8.3 below.

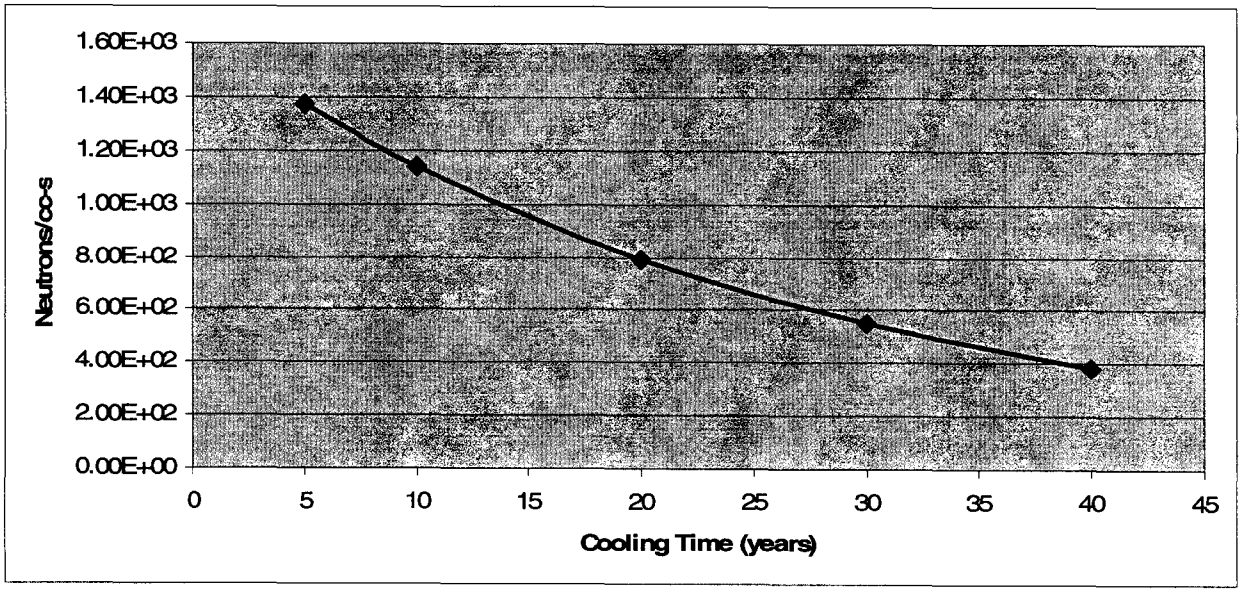

Figure 8.6 Neutron source term versus cooling time

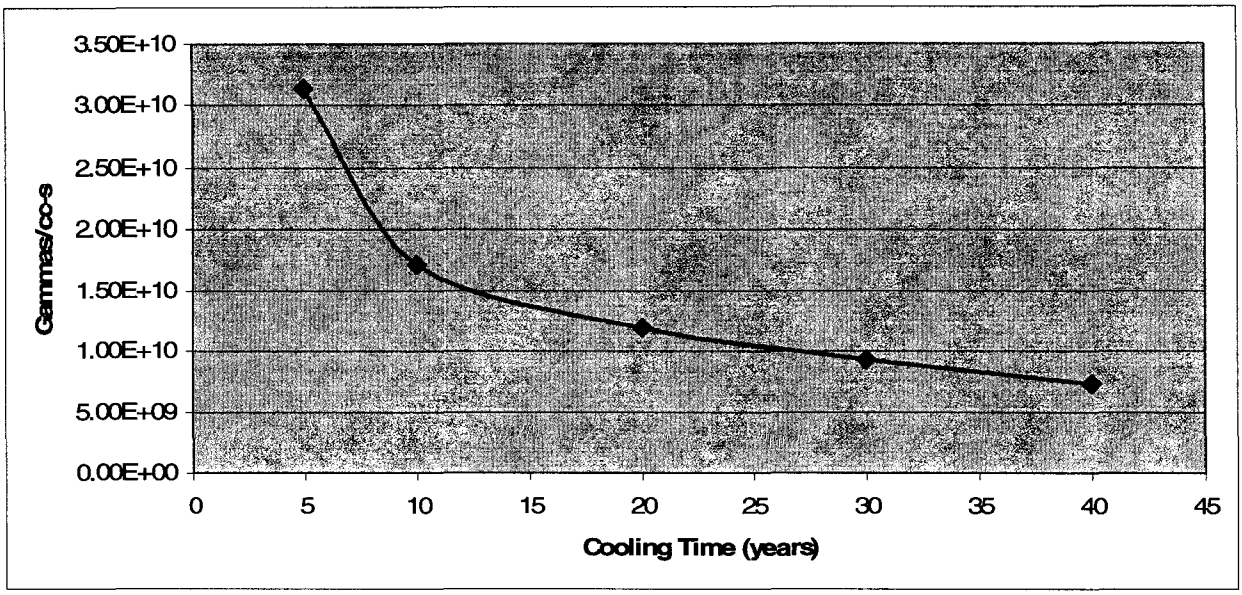

Figure 8.7 Gamma source term versus cooling time

Table 8.3 Source terms versus cooling time results

Cooling Time (years)	Neutrons/cc-sec	Gammas/cc-sec
5	1.37E+03	3.13E+10
10	1.14E+03	1.72E+10
20	7.87E+02	1.19E+10
30	5.48E+02	9.31E+09
40	3.85E+02	7.35E+09

The neutron and gamma source terms and the source energy spectra from the SAS2 calculations were used in SAS1 input decks to calculate neutron, gamma, and total fluxes at various points in the cask model. The SAS1 module provides a 1-D discrete-ordinates shielding analysis using XSDRNPM to calculate point dose rates.[25]

The model used for the dose rate calculations for the unmodified NUHOMS 24PL cask is shown in Figure 8.8. The design criteria state that the primary pressure boundary cannot be broken and therefore, the transducers have to be placed directly on both sides of the upper

stainless steel cover plate. To make room for the inside transducer and other components, a hole approximately 15cm in diameter and 4 cm deep will be bored into the lower stainless steel cover plate and the carbon steel/lead radiation shield. This hole will house the transducer, pressure sensor, and the other electronic components. The electronics must be connected to the thermocouples and thermopiles that are in the center of the cask so a shaft must be created that connects the electronics region to the cask interior. To avoid creating a collimated, unshielded beam leading from the interior to the electronics, the shaft for the wires will run diagonally from the bottom corner of the shield to the top center where the electronics will be. This is shown schematically in Figure 8.9 below.

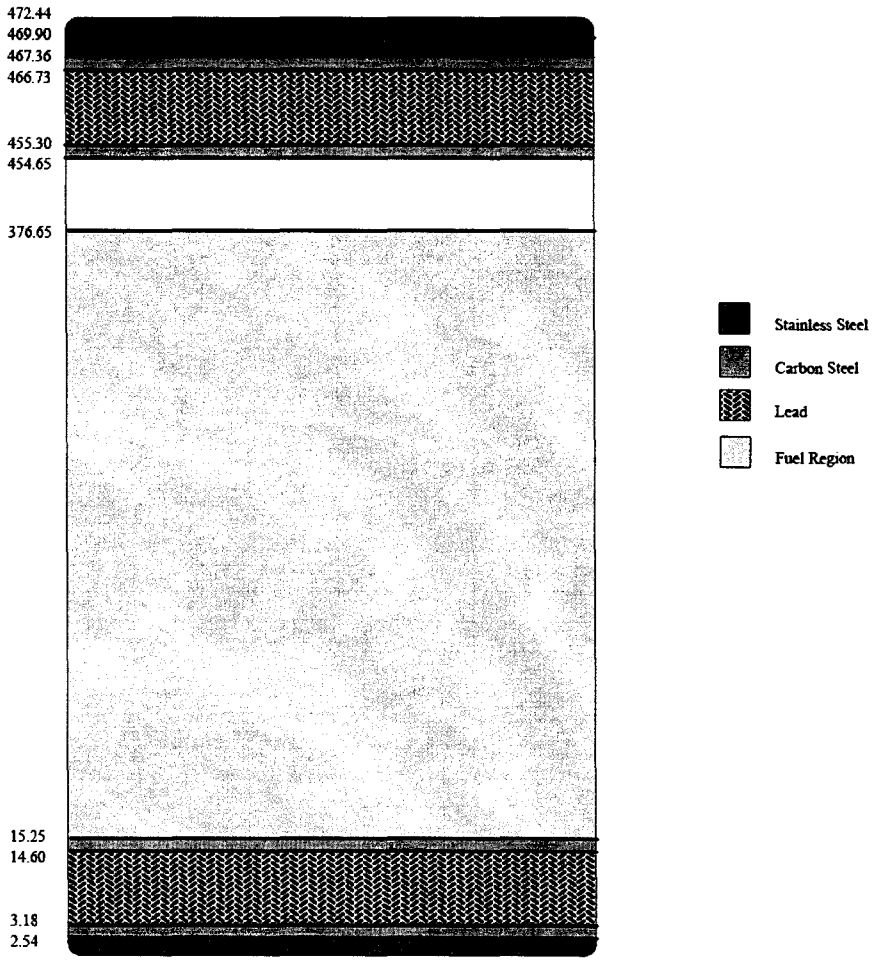

Figure 8.8 Unmodified cask design SAS1 model (units in cm)

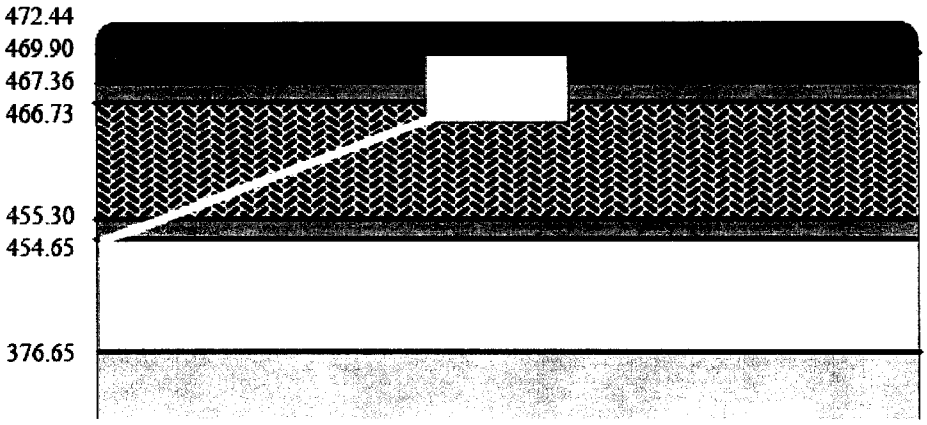

Figure 8.9 SAS1 Model of modified shield design (units in cm)

Using these models, SAS1 calculations were performed to determine the dose rates as a function of axial distance. These calculations were performed using the source spectra from the SAS2 calculations for 5, 10, 20, 30, and 40 years of cooling. A sample input deck for these SAS1 calculations is shown in Appendix Q. To show the effect of the electronics housing, Figures 8.10 and 8.11 compare dose rates as functions of distance into the shield for the normal and modified shield designs after 10 years of cooling. It shows that the removal of shield material significantly increases the dose on the outside of the shield for both neutron and gamma radiation. For gamma radiation, the dose rate outside of the cask is approximately 10 times higher for the modified shield design than for the unmodified while the neutron dose rates are relatively close. This is because the lead and steel of the shield attenuates the gammas much more effectively than neutrons.

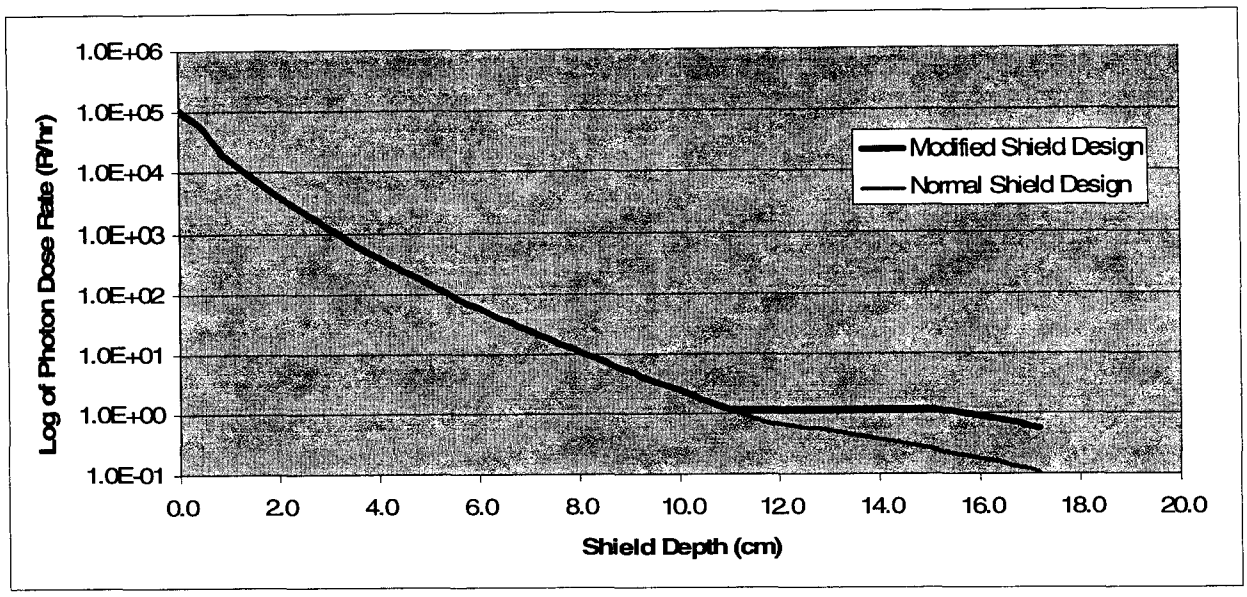

Figure 8.10 Log of gamma dose rate (R/hr) versus shield depth in the top of a NUHOMS 24PL cask

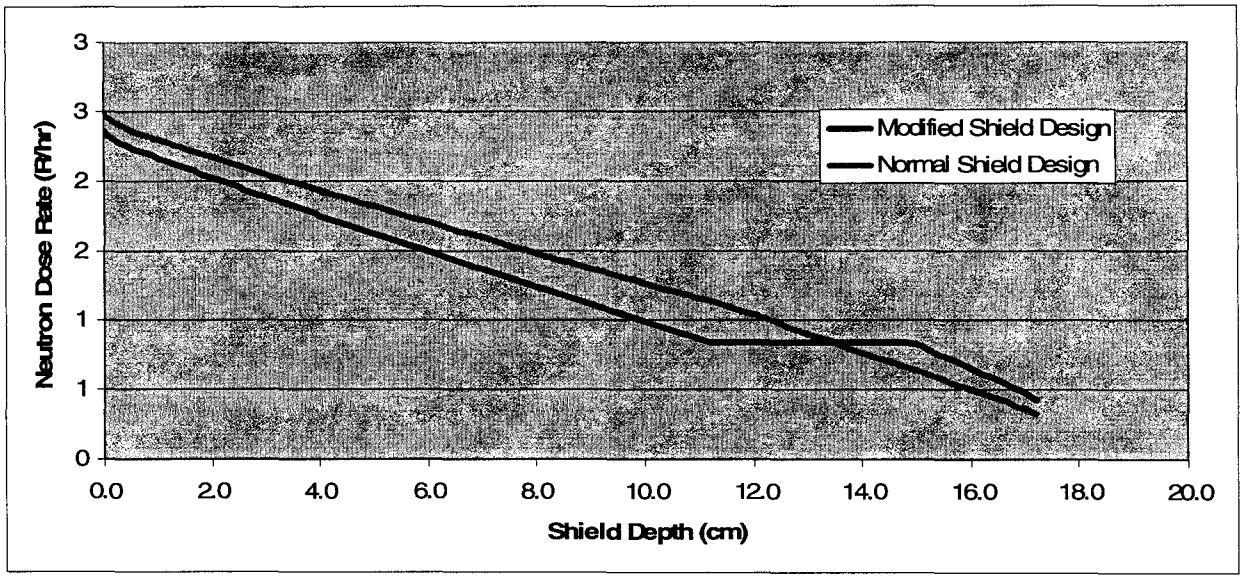

8.11 Neutron dose rate (R/hr) versus shield depth in the top of a NUHOMS 24PL cask

Calculations were also done to find the dose rate at certain points in the shield as a function of cooling time. In Figure 8.12, it is shown that total dose rate drops to 60% of its initial value within 5 years and drops to 10% in 40 years.

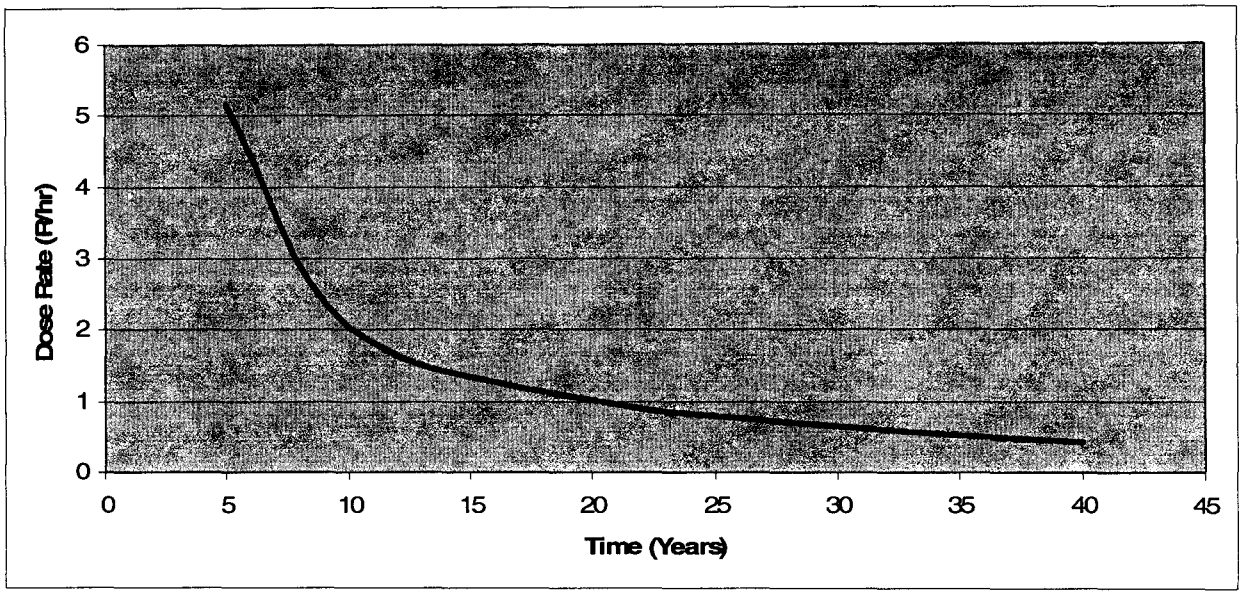

Figure 8.12 Dose rate (R/hr) versus cooling time in electronics region of modified shield design in a NUHOMS 24PL cask

To find accumulated dose at a certain point in the axial direction, a 6^{th} order polynomial fit is applied to a plot of dose rate versus time. The integral of the polynomial over the time desired yields a total accumulated dose for that point. This methodology was applied to Figure 8.12 and the total accumulated dose for the electronics was 0.363 megarads after 40 years of cooling. The design criteria state that the radiation-hardened electronics can withstand 1 MR, so this value is well below that limit. Also, the total accumulated dose calculation weights gamma and neutron doses equally even though electronics are relatively immune to neutron radiation

when compared to gamma radiation. Therefore, the total effective dose on the electronics will be even lower than 0.363 MR.

Dose rate as a function of cooling time was also calculated for the area just outside of the cask for the modified and normal shield designs. The plot is shown in Figure 8.13 below. This shows that the dose rate outside of the cask is initially almost 3 times higher for the modified cask than the normal cask, but that the dose rates converge after long cooling times.

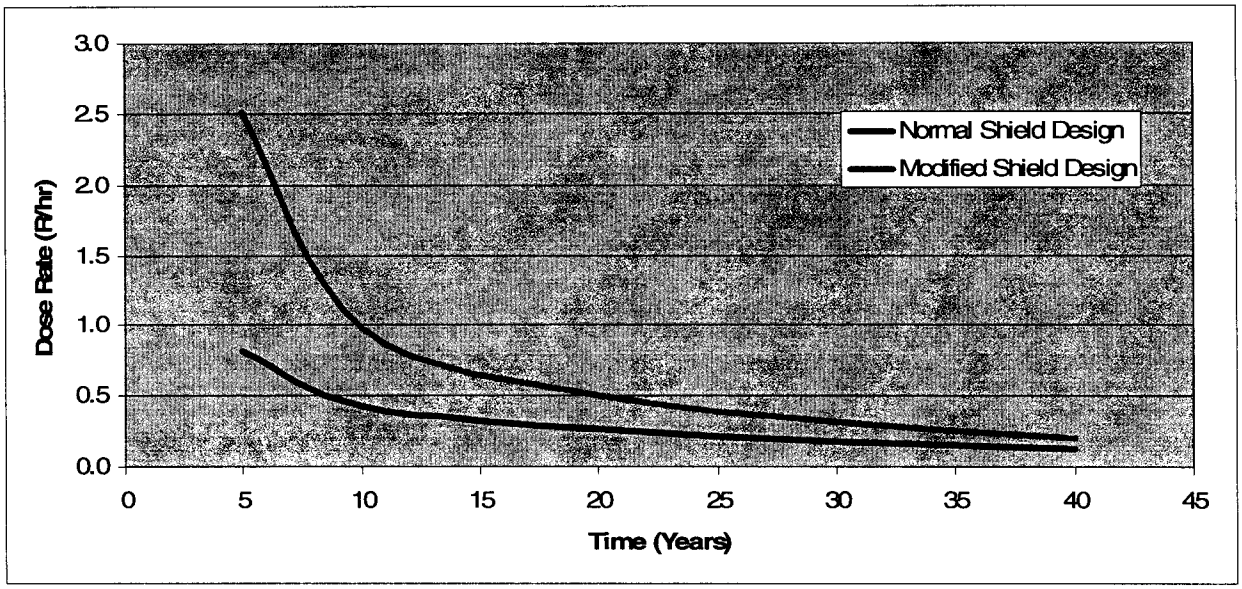

Figure 8.13 Dose rates (R/hr) versus cooling time outside of NUHOMS 24PL cask

Once again, polynomial fits were added to Figure 8.13 and their integrals taken to calculate total accumulated dose. The accumulated dose for outside the normal cask is 84.2 kR while the dose outside of the modified cask is 172.2 kR after 40 years of cooling. Although the modified cask dose is more than twice as high as the normal cask dose, one must remember that this modification only affects a small portion of the cask since only the center of the shield is affected by the inclusion of the electronics area. By weighting the doses with their relative areas

in the modified cask design, one can arrive at an area-averaged accumulated dose that would be more of an accurate way to judge the affect of the hole in the shield. These results are shown in Table 8.4 below.

Table 8.4 Area-averaged accumulated dose outside of cask

	Area (cm^2)	Dose (kR)	Average Dose (kR)
Modified	176.7	172.2	84.9
Normal	22698.6	84.2	

The area-averaged accumulated dose is 84.9 kR, while is just slightly over the unmodified cask dose of 84.2 kR. However, if one did not want to allow any increase in dose outside of the cask, a plate of lead the size of the area removed for the electronics could be welded either on the outside of the cask or on the inner side of the shield plug. If it were added to the inner side of the shield plug, not only would the dose rate outside of the cask be unchanged, but the dose absorbed by the electronics would be lowered as well.

9 External Data Transmission

The system to be designed is supposed to measure temperature and pressure conditions within the cask, transmit that information through the cask wall, and then record and analyze that information outside of the cask. However, once the information is out of the cask, it still has to be transmitted out of the Horizontal Storage Module (HSM) before it can be recorded or analyzed. The most obvious solution to this is to run a wire from the external transducer to a

receiver outside of the HSM. Although drilling a hole in the HSM for the wire would probably be acceptable, there are still problems with connecting the external transducer to a receiver. The electronic components of the measurement system are on the top end of the storage cask, and are therefore located at the back end of the HSM. This means that to connect a wire to the external transducer, a worker would have to physically attach the wire to the cask once it had been removed from the cask. Doing so would mean that the worker is subjected to a short dose of radiation as well as intense heat on the outside of the cask. Also, the wire would have to be kept away from the cask as it is pushed into the HSM to avoid severing the wire.[2]

Because of these difficulties in using wired data transmission, it is suggested that a wireless transmitter be used to send temperature and pressure data from the external transducer to a receiver outside of the HSM. Since the signal has to penetrate 2 feet of steel reinforced concrete, the signal will have to be in the radio frequency (RF) range. The signal should be in the lower part of the RF spectrum because higher frequencies are attenuated more readily as a function of barrier depth. In this range, there are many frequency bands that are available for license-free data transmission, like the 1800-1900 kHz band reserved for public use.[28]

The RF transmitter is a very common electrical component and one could be custom-made for this system. It would need to be radiation-hardened, because even though it is outside of the cask it will still be subjected to significant levels of neutron and gamma radiation. It will also have to be built to withstand the high temperatures of the cask wall.

In order to amplify and transmit the signal, the RF transmitter will have to have its own power source. Since it will be located in the sealed HSM, a photovoltaic cell will not be practical. A nuclear battery would fulfill the power and long lifetime requirements but would be prohibitively expensive. Therefore, a thermopile is the best solution. Since the HSM brings in

cool air from the bottom and vents the heated air from the top, the top of the cask will be hotter than the bottom[2]. The thermopile's hot junctions would therefore be placed on the top of the cask and the cold junctions on the bottom. The total number of thermocouples required in the thermopile would have to be determined after the power requirements of the RF transmitter are finalized.

10 System Design and Response

10.1 Design of Measurement System

The system discussed in the previous sections is designed for internal spent fuel dry storage cask data collection and transmission. Specifics of the cask and the system design criteria are discussed in Sections 2.0 and 3.0. The components to be included in the final product are: thermocouples, pressure sensors, thermopiles, a multiplexer, two transducers, a wireless RF transmitter with thermopiles, wireless RF receiver and an integrated circuit which contains an amplifier, voltage regulator, and voltage oscillator (Figure 10.1).

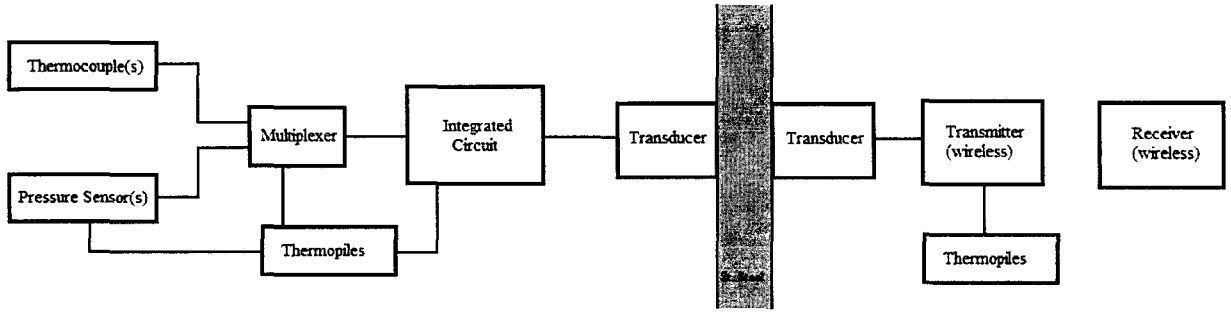

Figure 10.1 Layout of System Design

A multiplexer is included to decrease circuitry redundancies, lowering costs and raising efficiency. The multiplexer circuit, powered by the thermopiles, is designed to accept multiple inputs consecutively and after amplification, transmit the signal to the next device. The multiplexer selected for the system is the Analog Devices CMOS Analog Multiplexer ADG506A/ADG507A with 8 or 16 channel inputs which specifically states the ability to have temperature and pressure inputs (Appendix K and L)[30]. Approximately every 20 microseconds the multiplexer input switches to the next channel, and the signal is received for about 1 millisecond. The multiplexer will connect to the integrated circuit, which contains the operational amplifier, voltage-controlled oscillator, and voltage regulator.

The signal transmitted by the multiplexer is received by the operational amplifier, which is designed to increase an incoming signal by a specific amount of gain. The amplifier selected due to provision of cold junction compensation is the Analog Devices monolithic thermocouple amplifier AD594/AD595 (Appendix M)[31].

The signal produced by the amplifier feeds directly into the voltage-controlled oscillator (VCO). The VCO produces an oscillating signal at a frequency that is proportional to the received voltage. Selected for use in this system is the Texas Instruments SN74LS624N voltage-controlled oscillator (Appendix N and O)[32].

In order to maintain a constant level of operating voltage to the amplifier and the VCO, a voltage regulator is employed. The device chosen for this application is the National Semiconductor LM7805 3-terminal positive voltage regulator[29]. This voltage regulator provides a 5 volt output and has the ability to limit the output current, protecting other equipment, with internal short circuiting capability.

10.2 System Experiment

In order to prove the feasibility of the proposed design, an experiment was performed using a modified setup due to equipment availability. The setup included: a hot-plate, thermocouple, power supply (batteries), the integrated circuit, two transducers, a 3/8 inch (9.53 mm) stainless steel plate, an oscilloscope, and a device to read the output frequency (Figure 10.2). Because one thermocouple was used and no pressure sensor was available, a multiplexer was unnecessary between the thermocouple and the amplifier. Also as the experiment was completed at standard room temperature, batteries were used to generate power for the integrated circuit instead of the proposed thermopiles. The transducers were coupled to the stainless steel plate with petroleum jelly and were clamped in place to maintain constant pressure and contact with the plate. The signal received through the steel by the transducer was transmitted to a digital display for frequency readout and to an oscilloscope for visual confirmation.

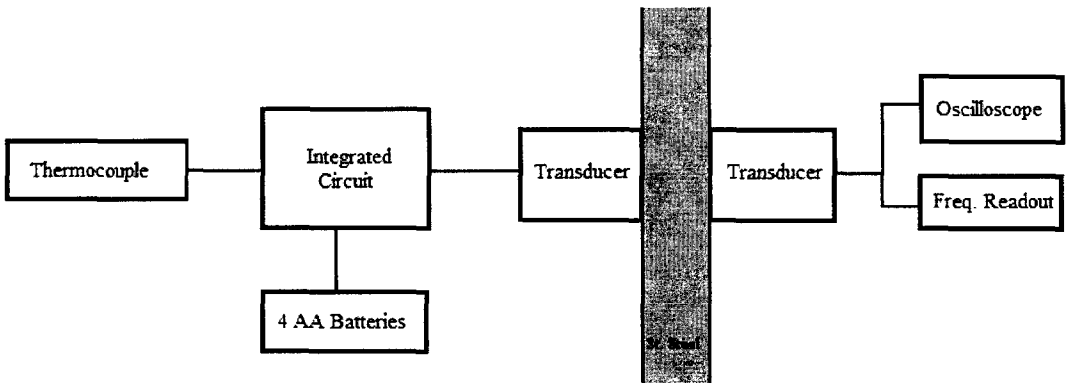

Figure 10.2 Layout of Experimental Setup

The integrated circuit contains all of the components previously described in Section 10.1, with the addition of bypass capacitors (Figure 10.3)

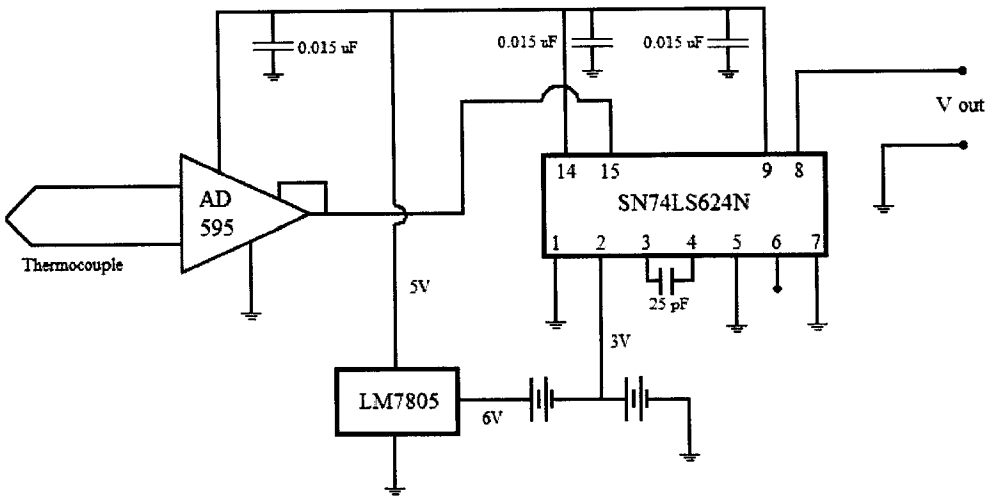

Figure 10.3 Experimental Circuit Diagram

Specifically the experiment included measurement of the change in the frequency of the produced signal as the temperature applied to the thermocouple increased (Table 10.1).

Table 10.1 Frequency produced by VCO versus temperature of thermocouple

Temperature (°C)	Frequency (MHz)
23.89	2.169
102.22	4.7
126.67	5.36
133.33	5.219
167.22	7.369
164.44	7.153
200.00	8.4078
338.33	7.491*
377.78	7.229*

* Instability of the oscillator occurred

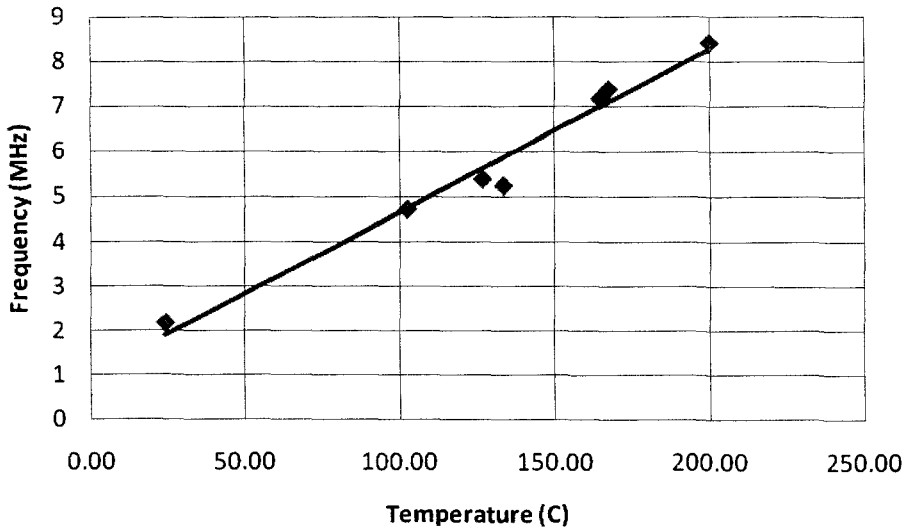

Figure 10.4 Frequency versus Thermocouple Temperature

The results indicate the ability for the voltage-controlled oscillator to increase the frequency with temperature in an approximately linear fashion. These results provide evidence that the proposed system is functional and capable of expected results.

11 Future Work

Several factors require further attention for this project to become a functional device in industry. Further data is required for each of the individual portions of the design, the data transference away from the cask, and the cost analysis of the proposed system.

First, data should be gathered to improve each portion of the design. Each piece should be able to withstand temperature and dose amounts for the lifetime of the cask while maintaining functionality. This data should include the durability of the materials of each device and any couplant used within the design. The circuitry input and output should be optimized, and studied for environmental effects. More data should be gathered on the possibility of a nuclear battery for the system also. Dose calculations should also performed for longer cooling times up to 100 years.

More specific details should be analyzed for transmitting the data to a location away from the cask using the radio frequency transmitter. A specific design should be obtained that is heat resistant and radiation hardened. The power requirements needed to operate the RF transmitter should be established. From this knowledge a thermopile can be specifically designed to power the device. A specific design will also be required for the RF receiver that can record the temperature and pressure data. Testing should be performed on the external transducer and the signal to the RF transmitter and then RF receiver. Alternative methods for transmitting data away from the cask should be researched further and tested.

Also, a detailed cost analysis should be performed on the materials required, the manufacturing costs, funds for further research and development, and installation. The cost

analysis should determine the benefit of the product and the data it produces compared to the savings gained from the system's data.

References

1. Nuclear Regulatory Commission, "Dry Cask Storage" http://www.nrc.gov/waste/spent-fuel-storage/dry-cask-storage.html February 2007
2. Transnuclear Inc. *The NUHOMS Modular Concrete Shielded Dry Storage System*, June 2007
3. Transnuclear Inc. *Updated Final Safety Analysis Report for the Standardized NUHOMS Horizontal Modular Storage System for Irradiated Nuclear Fuel*, January 2006
4. Dataforth Corp. http://www.dataforth.com/ Dataforth Corp 3331 E Hemisphere Loop Tucson, Arizona
5. Omega http://www.omega.com/temperature/Z/zsection.asp Omega Engineering Inc.
6. Ceramawire Manufacture of Ceramic Wire http://www.ceramawire.com/techspec.html 786 Pitts Chapel Rd. Elizabeth City, NC
7. Kester, Walt. Strain, Pressure, and Flow Measurements. http://www.analog.com/UploadedFiles/Associated_Docs/3246356179450253207484365249943576531814906121654022 3Fsect4.PDF
8. Wilson, Jon. "Pressure Measurement: Principles and Practice". *Sensors.* January 1, 2003.
9. Omega, *High Pressure Transducers* http://www.omega.com/Pressure/pdf/PX1004.pdf
10. NTD Resource Center "Introduction to Ultrasonic Testing" http://www.ndt-ed.org/EducationResources/CommunityCollege/Ultrasonics/cc_ut_index.htm
11. Olympus, Panametrics-NDT *Ultrasonic Transducers Technical Notes* http://www.olympusndt.com/data/File/panametrics/UT-technotes.en.pdf
12. Olympus, Panametrics-NDT *Phased Array Tutorial* http://www.olympusndt.com/en/ndt-tutorials/phased-array/
13. Socki, Jim "Quartz Crystal Oscillator Training Seminar" November 2000, http://www.ndt-ed.org/EducationResources/CommunityCollege/Ultrasonics/EquipmentTrans/PiezoelectricEffect.ppt
14. Olympus, Panametrics-NDT *Ultrasonic Transducers for Nondestructive Testing* http://www.olympusndt.com/data/File/panametrics/panametrics-UT.en.pdf

15. Olympus "Corrosion Gaging with Dual Element Transducers" http://www.olympusndt.com/en/ndt-application/183-id.209715222.html
16. The Physical and Theoretical Chemisty Laboratory, Oxford University, *Safety data for petroleum jelly* http://msds.chem.ox.ac.uk/PE/petroleum_jelly.html
17. Mallinckrodt Chemicals, J.T. Baker, Jan. 2006 *MSDS Magnesium Oxide* http://www.jtbaker.com/msds/englishhtml/M0182.htm
18. Kirk, K.J., Scheit, C.W., Schmarje, N., *High-temperature acoustic emission tests using lithium niobate piezocomposite transducers* www.ndt.net/search/docs.php3?id=4551
19. Akgun, U., Onel, Y., Insight, Volume 49 Number 3 March 2007 *Radiation-Hard Quartz Čerenkov Calorimeters* www.physics.uiowa.edu/~u**akgun**/FILES/calor2006_**onel**.pdf
20. Ionizing Radiation and Polymers Ed. Betz, N., Le Moel, A., Elsevier North Holland, September 2000 Briskman, B.A. *Radiation effects in thermal properties of polymers. An analytical review. I. Polyethylene*
21. Ionizing Radiation and Polymers Ed. Güven, O., Elsevier North Holland, September 2006 Kakigi, T., Oshima, A., Miyoshi, N., Katsuyoshi, M., Fujii, K., Mitani, N, Urakawa, T., Sato, Y., Matsuura, A., Li, J., Miura, T., Katoh, E., Washio, M. *Study on chemical structures of poly (tetrafluoreoethylene-co-perfluoroalkylvinylether) by soft-EB irradiation in solid and molten state*
22. Ionizing Radiation and Polymers Ed. Güven, O., Elsevier North Holland, September 2006 Burillo, G., Briones, M., Adem, E. *IPN's of acrylic acid and N-isopropylacrylamide by gamma and electron beam irradiation*
23. Neely Industries, Dow Corning 1997 *Information about High viscosity silicone fluids* http://www.neelyindustries.com/pdf/200high.pdf
24. Thermoelectric Technical Reference, Ferro Tec http://www.ferrotec.com/technology/thermoelectric/thermalRef01.php
25. Thermo-Pile,ThermoModule & Thermocontroller http://www.hexagold.com/Sensors/ThermoPile/thermopile.html
26. The Thermopile http://scholar.lib.vt.edu/theses/available/etd-8497-205315/unrestricted/chap2.pdf

27. Introduction to Thermocouples, Capgo
http://www.capgo.com/Resources/Temperature/Thermocouple/Thermocouple.html

28. U.S. Department of Commerce, National Telecommunications and Information Administration, Office of Spectrum Management, United States Frequency Allocations - The Radio Spectrum, October 2003.

29. National Semiconductor, *LM341/LM78MXX Series 3-Terminal Positive Voltage Regulators* July 1999

30. Analog Devices, *CMOS 8-/18- Channel Analog Multiplexers (ADG506A/ADG507A)*, 1998

31. Analog Devices, *Monolithic Thermocouple Amplifiers with Cold Junction Compensation (AD594/AD595)*, 1999

32. Texas Instruments, *SN54LS624 thru SN54LS629, SN74LS624 thru SN74LS629 Voltage-Controlled Oscillators*, rev. March 1986

OLYMPUS

Tel: 781- 419-3900
www.olympusndt.com

TRANSDUCER DESCRIPTION

PART NO.: C109
SERIAL NO.: 614676
DESIGNATION: CONTACT

FREQUENCY: 5.00 MHz
ELEMENT SIZE: .5 in. DIA.

TEST INSTRUMENTATION

PULSER/RECEIVER: PANAMETRICS 5052UA #6
DIGITAL OSCILLOSCOPE: LeCroy LC564A / SN: LC56410253
TEST PROGRAM: TP103-3 VER. 10814F
CABLE: RG 174/U LENGTH: 4FT

TEST CONDITIONS

PULSER SETTING: ENERGY: 1 ; DAMPING: 50
RECEIVER SETTING: ATTN: 38dB ; GAIN: 20dB
TARGET: 2.0 IN STEEL
JOB CODE: TP200

MEASUREMENTS PER ASTM E1065

WAVEFORM DURATION:
-14DB LEVEL --- 0.328 US
-20DB LEVEL --- 0.356 US
-40DB LEVEL --- 0.684 US

SPECTRUM MEASURANDS:
CENTER FREQ. ------ 5.01 MHz
PEAK FREQUENCY -- 5.14 MHz
-6DB BANDWIDTH --- 82.62 %

COMMENTS:

** ACCEPTED

TECHNICIAN (7)

DATE: 01-18-2008

SIGNAL WAVEFORM

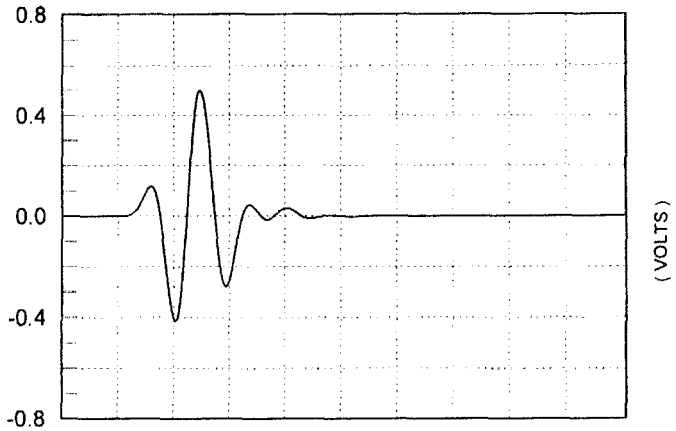

(.2 USEC / DIVISION)

FREQUENCY SPECTRUM

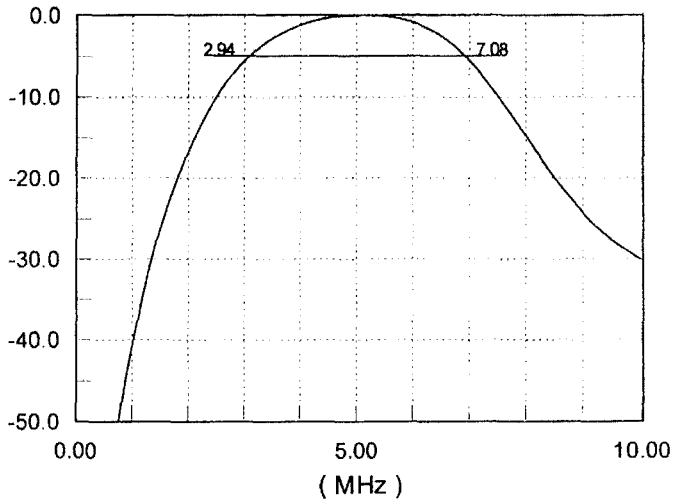

PANAMETRICS-NDT

Appendix B: Acoustic Properties of Materials[11]

Acoustic Properties of Materials

Material	Longitudinal Velocity		Shear Velocity		Acoustic Impedance
	(in/μs)*	(m/s)	(in/μs)*	(m/s)	(Kg/m²s x 10^6)
Acrylic resin (Perspex®)	0.107	2,730	0.056	1,430	3.22
Aluminum	0.249	6,320	0.123	3,130	17.06
Beryllium	0.508	12,900	0.350	8,890	23.5
Brass, naval	0.174	4,430	0.083	2,120	37.30
Cadmium	0.109	2,790	0.059	1,500	24.02
Columbium	0.194	4,920	0.083	2,100	42.16
Copper	0.183	4,660	0.089	2,260	41.61
Glycerine	0.076	1,920	—	—	2.42
Gold	0.128	3,240	0.047	1,200	62.60
Inconel®	0.29	5,920	0.119	3,020	49.47
Iron	0.232	5,900	0.127	3,230	45.43
Iron, cast					
(slow)	0.138	3,500	0.087	2,200	25.00
(fast)	0.220	5,600	0.126	3,220	40.00
Lead	0.085	2,160	0.028	700	24.49
Manganese	0.193	4,880	0.093	2,350	34.44
Mercury	0.057	1,450	—	—	19.88
Molybdenum	0.246	6,250	0.132	3,350	63.75
Motor Oil (SAE 20 or 30)	0.069	1,740	—	—	1.51
Nickel, pure	0.222	5,630	0.117	2,960	49.99
Platinum	0.156	3,960	0.066	1,670	84.74
Polyamide, (nylon, Perlon®)					
(slow)	0.087	2,200	0.043	1,100	.40
(fast)	0.102	2,600	0.047	1,200	3.10
Polystyrene	0.092	2,340	—	—	2.47
Polyvinylchloride, PVC, hard	0.094	2,385	0.042	1,060	3.35
Silver	0.142	3,600	0.063	1,590	37.78
Steel, 1020	0.232	5,890	0.128	3,240	45.63
Steel, 4340	0.230	5,850	0.128	3,240	45.63
Steel, 302	0.223	5,680	0.123	3,120	45.45
austenitic stainless Steel, 347	0.226	5,740	0.122	3,090	45.40
austenitic stainless Tin	0.131	3,320	0.066	1,670	24.20
Titanium, TI150A	0.240	6,100	0.123	3,120	27.69
Tungsten	0.204	5,190	0.113	2,870	99.72
Uranium	0.133	3,370	0.078	1,980	63.02
Water (20°C)	0.058	1,480	—	—	1.48
Zinc	0.164	4,170	0.095	2,410	29.61
Zirconium	0.183	4,650	0.089	2,250	30.13

* Conversion Factor: 1 m/s = 3.937×10^{-2} in/μs

Source: Nondestructive Testing Handbook 2nd Edition Volume 7
Ultrasonic Testing ASNT 1991 ed Paul McIntire

Appendix C: Near Field Lengths for 1020 carbon steel and 347 aus. SS

	St 1020		Aus. SS 347	
	Longitudinal		Longitudinal	
f (Hz)	c(m/s)	N (mm)	c (m/s)	N (mm)
500000	5890	3.42	5740	3.51
1000000		6.85		7.02
1500000		10.27		10.54
2000000		13.69		14.05
2100000		14.38		14.75
2200000		15.06		15.45
2300000		15.75		16.16
2400000		16.43		16.86
2500000		17.11		17.56
2600000		17.80		18.26
2700000		18.48		18.97
2800000		19.17		19.67
2900000		19.85		20.37
3000000		20.54		21.07
4000000		27.38		28.10
5000000		34.23		35.12
7500000		51.34		52.69
10000000		68.46		70.25
15000000		102.69		105.37

Appendix D: Values obtained using liquid silicone with 3/8 inch plate

TEST 1A						
Vpp = 6.0	Liquid Silicone	dimethylpolysiloxane				
Freq (MHz)		**Volts**	**Fraction of Signal**	**A1/A2**	**(-dB)**	**Comments**
2		0.175	0.029	34.29	-30.70	odd waveform
2.1		0.052	0.009	115.38	-41.24	odd waveform
2.2		0.064	0.011	93.75	-39.44	odd waveform
2.3		0.2	0.033	30.00	-29.54	odd waveform
2.4		0.06	0.010	100.00	-40.00	odd waveform
2.5		0.082	0.014	73.17	-37.29	odd waveform
2.6		0.26	0.043	23.08	-27.26	
2.7		0.072	0.012	83.33	-38.42	odd waveform
2.8		0.072	0.012	83.33	-38.42	odd waveform
2.9	peak values	0.096	0.016	62.50	-35.92	odd waveform
3		0.17	0.028	35.29	-30.95	two waveforms
3.1		0.09	0.015	66.67	-36.48	odd waveform

3.2		0.088	0.015	68.18	-36.67	odd waveform
3.3		0.076	0.013	78.95	-37.95	odd waveform
3.4		0.124	0.021	48.39	-33.69	
3.5	peak values	0.055	0.009	109.09	-40.76	high fluctuation level
3.6		0.076	0.013	78.95	-37.95	
3.7		0.175	0.029	34.29	-30.70	
3.8		0.102	0.017	58.82	-35.39	high fluctuation level
3.9		0.058	0.010	103.45	-40.29	
4		0.25	0.042	24.00	-27.60	
4.1		0.1	0.017	60.00	-35.56	
4.2		0.092	0.015	65.22	-36.29	
4.3		**0.62**	**0.103**	9.68	-19.72	
4.4		0.096	0.016	62.50	-35.92	
4.5		0.1	0.017	60.00	-35.56	
4.6	peak values	0.052	0.009	115.38	-41.24	
4.7		0.056	0.009	107.14	-40.60	odd waveform
4.8		0.112	0.019	53.57	-34.58	
4.9	peak values	0.1	0.017	60.00	-35.56	high fluctuation level
5		0.06	0.010	100.00	-40.00	odd waveform
5.1		0.11	0.018	54.55	-34.74	
5.2	peak values	0.136	0.023	44.12	-32.89	high fluctuation level
5.3		0.06	0.010	100.00	-40.00	
5.4		0.122	0.020	49.18	-33.84	
5.5		0.088	0.015	68.18	-36.67	
5.6		0.06	0.010	100.00	-40.00	
5.7		0.15	0.025	40.00	-32.04	
5.8		0.048	0.008	125.00	-41.94	
5.9		0.046	0.008	130.43	-42.31	
6	peak values	0.5	0.083	12.00	-21.58	high fluctuation level
6.1		0.042	0.007	142.86	-43.10	

6.2		0.044	0.007	136.36	-42.69	
6.3		0.044	0.007	136.36	-42.69	
6.4		0.042	0.007	142.86	-43.10	
6.5		0.036	0.006	166.67	-44.44	
6.6		0.072	0.012	83.33	-38.42	
6.7		0.028	0.005	214.29	-46.62	
6.8		0.031	0.005	193.55	-45.74	
6.9		0.046	0.008	130.43	-42.31	
7		0.024	0.004	250.00	-47.96	

Appendix E: Values obtained using petroleum jelly with 3/8 inch plate

TEST 1B						
Vpp = 6	petroleum jelly					
Freq (MHz)		**Volts**	**Fraction of Signal**	**A1/A2**	**(-dB)**	**Comments**
2	peak values	0.245	0.041	24.49	-27.78	odd waveform; high fluctuation
2.1		0.2	0.033	30.00	-29.54	odd waveform
2.2		0.14	0.023	42.86	-32.64	odd waveform
2.3	peak values	0.325	0.054	18.46	-25.33	high fluctuation level
2.4		0.17	0.028	35.29	-30.95	odd waveform
2.5		0.16	0.027	37.50	-31.48	
2.6	peak values	0.305	0.051	19.67	-25.88	
2.7		0.1	0.017	60.00	-35.56	
2.8		0.145	0.024	41.38	-32.34	
2.9		0.42	0.070	14.29	-23.10	
3	peak values	0.165	0.028	36.36	-31.21	odd waveform
3.1		0.17	0.028	35.29	-30.95	
3.2		0.22	0.037	27.27	-28.71	
3.3		0.155	0.026	38.71	-31.76	
3.4		0.2	0.033	30.00	-29.54	
3.5	peak values	0.1	0.017	60.00	-35.56	high fluctuation level
3.6		0.14	0.023	42.86	-32.64	
3.7		0.26	0.043	23.08	-27.26	
3.8	peak values	0.108	0.018	55.56	-34.89	
3.9		0.116	0.019	51.72	-34.27	
4		0.35	0.058	17.14	-24.68	
4.1		0.15	0.025	40.00	-32.04	
4.2		0.155	0.026	38.71	-31.76	
4.3		**0.58**	**0.097**	10.34	-20.29	
4.4		0.2	0.033	30.00	-29.54	
4.5		0.17	0.028	35.29	-30.95	
4.6	peak values	0.5	0.083	12.00	-21.58	
4.7		0.15	0.025	40.00	-32.04	

4.8		0.21	0.035	28.57	-29.12	
4.9	peak values	0.084	0.014	71.43	-37.08	
5		0.116	0.019	51.72	-34.27	odd waveform
5.1		0.215	0.036	27.91	-28.91	
5.2	peak values	0.2	0.033	30.00	-29.54	
5.3		0.13	0.022	46.15	-33.28	
5.4		0.2	0.033	30.00	-29.54	
5.5		0.195	0.033	30.77	-29.76	
5.6		0.1	0.017	60.00	-35.56	
5.7		0.225	0.038	26.67	-28.52	
5.8		0.16	0.027	37.50	-31.48	
5.9		0.1	0.017	60.00	-35.56	
6		0.34	0.057	17.65	-24.93	
6.1		0.044	0.007	136.36	-42.69	
6.2		0.068	0.011	88.24	-38.91	
6.3	peak values	0.1	0.017	60.00	-35.56	high fluctuation level
6.4		0.06	0.010	100.00	-40.00	
6.5		0.042	0.007	142.86	-43.10	
6.6	peak values	0.076	0.013	78.95	-37.95	high fluctuation level
6.7		0.064	0.011	93.75	-39.44	
6.8		0.064	0.011	93.75	-39.44	
6.9		0.104	0.017	57.69	-35.22	
7		0.052	0.009	115.38	-41.24	

Appendix F: Values obtained using Magnesium hydroxide with 3/8 inch plate

TEST 1C				
Vpp = 6	Mg(OH)2			
Freq (MHz)	**Volts**	**Fraction of Signal**	**A1/A2**	**(-dB)**
3	0.175	0.029	34.29	-30.70
3.1	0.175	0.029	34.29	-30.70
3.2	0.16	0.027	37.50	-31.48
3.3	0.175	0.029	34.29	-30.70
3.4	0.218	0.036	27.52	-28.79
3.5	0.175	0.029	34.29	-30.70
3.6	0.17	0.028	35.29	-30.95
3.7	0.275	0.046	21.82	-26.78
3.8	0.21	0.035	28.57	-29.12
3.9	0.145	0.024	41.38	-32.34
4	0.31	0.052	19.35	-25.74
4.1	0.23	0.038	26.09	-28.33
4.2	0.19	0.032	31.58	-29.99
4.3	0.37	**0.062**	16.22	-24.20
4.4	0.225	0.038	26.67	-28.52
4.5	0.19	0.032	31.58	-29.99
4.6	0.27	0.045	22.22	-26.94
4.7	0.155	0.026	38.71	-31.76

4.8	0.24	0.040	25.00	-27.96
4.9	0.19	0.032	31.58	-29.99
5	0.075	0.013	80.00	-38.06
5.1	0.125	0.021	48.00	-33.62
5.2	0.11	0.018	54.55	-34.74
5.3	0.15	0.025	40.00	-32.04

Appendix G: Values obtained using liquid silicone with 6/8 inch plate

TEST 2A				
Vpp:	6	Liquid silicone		
Freq (MHz)	Volts	Fraction of Signal	A1/A2	(-dB)
1.7	0.064	0.011	93.75	-39.44
1.8	0.044	0.007	136.36	-42.69
1.9	0.052	0.009	115.38	-41.24
2	0.066	0.011	90.91	-39.17
2.1	0.04	0.007	150.00	-43.52
2.2	0.042	0.007	142.86	-43.10
2.3	0.068	0.011	88.24	-38.91
2.4	0.056	0.009	107.14	-40.60
2.5	0.04	0.007	150.00	-43.52
2.6	0.056	0.009	107.14	-40.60
2.7	0.088	0.015	68.18	-36.67
2.8	0.05	0.008	120.00	-41.58
2.9	0.048	0.008	125.00	-41.94
3	0.07	0.012	85.71	-38.66
3.1	0.06	0.010	100.00	-40.00
3.2	0.048	0.008	125.00	-41.94
3.3	0.054	0.009	111.11	-40.92
3.4	0.056	0.009	107.14	-40.60
3.5	0.05	0.008	120.00	-41.58
3.6	0.044	0.007	136.36	-42.69
3.7	0.04	0.007	150.00	-43.52
3.8	0.036	0.006	166.67	-44.44
3.9	0.04	0.007	150.00	-43.52
4	0.035	0.006	171.43	-44.68
4.1	0.026	0.004	230.77	-47.26
4.2	0.028	0.005	214.29	-46.62
4.3	0.028	0.005	214.29	-46.62
4.4	0.0175	0.003	342.86	-50.70
4.5	0.017	0.003	352.94	-50.95
4.6	0.0235	0.004	255.32	-48.14
4.7	0.0175	0.003	342.86	-50.70
4.8	0.011	0.002	545.45	-54.74
4.9	0.0175	0.003	342.86	-50.70
5	0.0155	0.003	387.10	-51.76
5.1	0.011	0.002	545.45	-54.74
5.2	0.008	0.001	750.00	-57.50

5.3	0.015	0.003	400.00	-52.04
5.4	0.009	0.002	666.67	-56.48
5.5	0.0065	0.001	923.08	-59.30
5.6	0.0065	0.001	923.08	-59.30
5.7	0.0065	0.001	923.08	-59.30
5.8	0.005	0.001	1200.00	-61.58
5.9	0.0055	0.001	1090.91	-60.76
6	0.0045	0.001	1333.33	-62.50

Appendix H: Voltage response due to addition of rough plates

TEST 3A				
Amp = 3.0	**Vpp = 6.00**	Vrms = 1.06		
Freq (MHz)	**Thickness (mm)**	**Volts**	**Fraction of Signal**	**Comments**
4.3	9.525	0.009	0.0015	1 unpolished plate
	19.05	0.0012	0.0002	extremely difficult to read

Appendix I: Voltage response due to addition of smooth plates

TEST 3B				
Amp = 3.0	**Vpp = 6.00**	Vrms = 1.06		
Freq (MHz)	**Thickness (inch)**	**Volts**	**Fraction of Signal**	**Comments**
4.3	9.525	0.64	0.1067	1 polished plate
	19.05	0.084	0.0140	1 polished + 1 unpolished
	28.575	0.013	0.0022	

Appendix J: Voltage response to Offset obtained using liquid silicone with 3/8 inch plate

TEST 2A					
Amp = 3.0	**Vpp = 6.0**				
Frequency	**Offset (mm)**	Volts	Fraction of Signal	A1/A2	(-dB)
4.3	0	0.37	0.062	16.22	-24.20
	2	0.36	0.060	16.67	-24.44
	4	0.15	0.025	40.00	-32.04
	6	0.1	0.017	60.00	-35.56
	7.5	0.075	0.013	80.00	-38.06
	12	0.05	0.008	120.00	-41.58
	15	0.05	0.008	120.00	-41.58
	18	0.04	0.007	150.00	-43.52

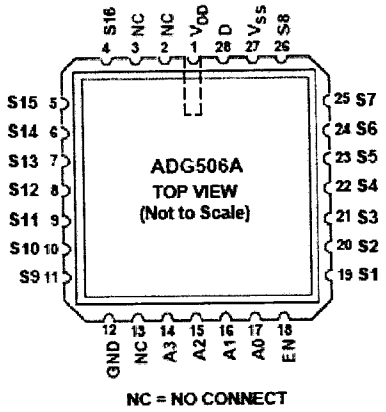

Appendix K: Pin Configuration of Multiplexer[30]

Analog Devices, *CMOS 8-/18- Channel Analog Multiplexers (ADG506A/ADG507A)*, 1998

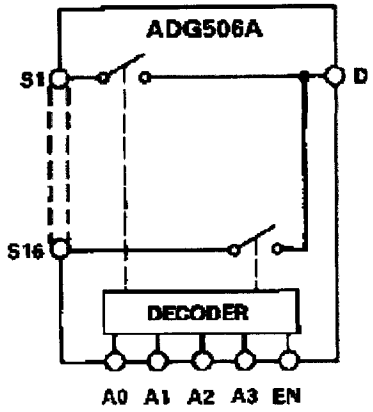

Appendix L: Functional Block Diagram of Multiplexer[30]

Analog Devices, *CMOS 8-/18- Channel Analog Multiplexers (ADG506A/ADG507A)*, 1998

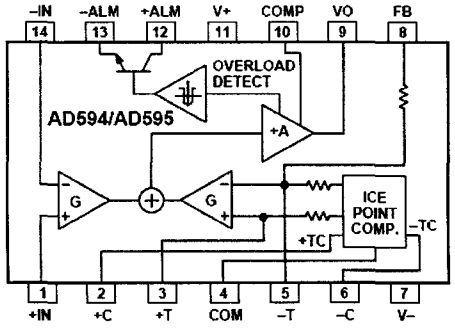

Appendix M: Functional Block Diagram of Operational Amplifier[31]

Analog Devices, *Monolithic Thermocouple Amplifiers with Cold Junction Compensation (AD594/AD595)*, 1999

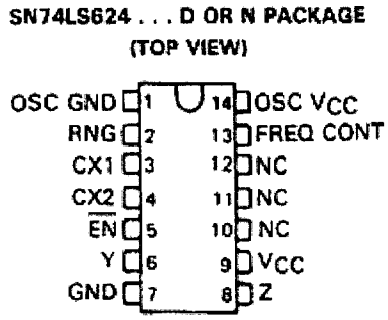

Appendix N: Voltage-Controlled Oscillator Pin Configuration[32]

Texas Instruments, *SN54LS624 thru SN54LS629, SN74LS624 thru SN74LS629 Voltage-Controlled Oscillators*, rev. March 1986

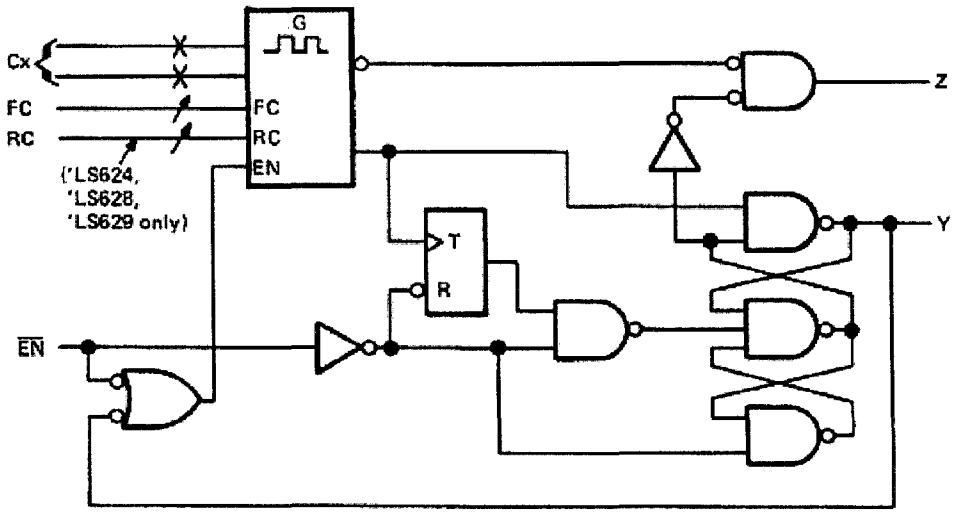

Appendix O: Voltage-Controlled Oscillator Logic Diagram

Appendix P: SAS2 Sample Input Deck

```
=sas2 parm='skipcellwt,runshipcask'
Design Basis, 20 Years Cooling
44GROUPNDF5                    LATTICECELL
uo2         1 den=10.96 1.0 1010 92235 4.0 92238 96.0 END
zirconium   2            1.0  730                        END
h2o         3 den=.637   1.0  600                        END
h2o         4           1.e-20                          END
ss304       5             1.0                           END
END COMP
SQUAREPITCH 1.444272  0.9487 1  3  1.0922 2  0.9652 0 END
 NPIN/ASSM=208 FUELNGTH=361.4 NCYCLES=1 NLIB/CYC=8
PRINTLEVEL=4    INPLEVEL=1    NUMZTOTAL=2            END
POWER=20       BURN=1068.75 DOWN=7304.8 END
27n-18couple tempcask(k)=325 numzones=4 dryfuel=yes END
 4     67.0452    5     68.8     4     83.7565    5      85.344
zone=1 fuelbndl=24 end
end
```

Appendix Q: SAS1 Sample Input Deck

```
=sas1            PARM=SIZE=999999
Modified shield design axial calculations, 30 years cooling
27n-18couple                   LATTICECELL
uo2         1 den=10.96 1.0 1010 92235 1.0 92238 99.0 END
zirconium   2 1.0 730 END
h2o         3 den=.637 1.0 600 END
h2o 4 1.e-20 end
ss304 5 1.0 end
CARBONSTEEL 6 1.0 end
LEAD 7 1.0 end
ss304 8 0.25 end
W 9 den=19.35 1.0 400 74184 100.0 end
B4C 10 1.0 end
END COMP
SQUAREPITCH 1.444272  0.9487 1  3  1.0922 2  0.9652 0 END
more data dy=134.09 dz=134.09 end
end
LAST
Shielding of 1 Ci 2 MeV neutron source
disc vacuum
    5       2.54          12          0
    6       3.175          3          0
    7       14.605        57          0
    6       15.24         76          0
  500       376.64      1883         -1      0 0.          5.4808e2 9.3101e9
    4       454.66       390          0
    6       455.295        3          0
    7       465.9         53          0
    4       469.9         19          0
    5       472.44        12          0
```

```
END ZONE
1.0860E+01
1.1790E+02
1.3290E+02
6.9290E+01
8.5840E+01
8.5700E+01
3.9330E+01
5.8060E+00
4.1600E-01
3.0760E-02
2.4220E-03
1.7060E-04
2.6710E-05
5.2860E-06
5.9820E-07
1.7580E-07
5.6660E-08
4.0580E-08
5.7400E-08
9.3480E-08
1.3710E-08
1.5940E-08
1.5220E-08
4.1290E-09
1.2160E-09
8.6430E-10
2.3030E-10
3.1260E-01
1.4730E+00
7.5100E+00
1.8720E+01
5.5490E+01
6.7130E+02
1.3750E+04
2.6930E+05
4.4720E+06
4.8580E+07
3.6320E+07
4.8570E+09
7.7300E+07
1.0520E+08
1.5390E+08
4.9650E+08
8.2150E+08
2.7090E+09
READ XSDOSE
  67.0452
END
```